**MEASURING EEDF IN GAS DISCHARGE PLASMAS, (REVIEW),** NATO ASI Series, E, Appl. Sci. V. 176, pp 95-134, Plasma Surface Interaction and Processing of Materials, Kluwer Acad. Publishers (1990).

# MEASURING EEDF IN GAS DISCHARGE PLASMAS

(Review)

Valery A. Godyak*

GTE Products Corporation
Danvers, MA. USA

*Present Address:
GTE Laboratories, Inc.
40 Sylvan Road
Waltham, MA. 02254, USA

# MEASURING EEDF IN GAS DISCHARGE PLASMAS

(Review)

V. A. GODYAK*

GTE Products Corporation
Danvers, MA, 01923 USA

## 1. INTRODUCTION

The plasma probe diagnostic is the primary technique for obtaining information concerning the plasma parameters in low pressure gas discharges. In its classical application, known as the Langmuir technique, the probe method allows us to find the basic plasma parameters: the plasma density and the electron temperature. Once these parameters are obtained, we have enough information for the calculation of plasma hydrodynamic processes. The problem arises when one tries to calculate the rates of non-elastic interactions of the plasma electrons with molecules and ions using the measured electron temperature of the low energy electrons.

Low pressure discharge plasmas are non-equilibrium plasmas: electrons are not in equilibrium with other plasma components, nor with the electron ensemble itself. This means that the electron energy distribution function (EEDF) is non-Maxwellian, and as a result, the concept of an electron temperature is not fully applicable. The electron temperature deduced from probe measurements can characterize no more than the mean electron energy, and cannot be used for calculations of excitation or ionization rates, unless evidence of a Maxwellian EEDF exists.

Fortunately, one can measure the EEDF using a Langmuir probe. This was demonstrated by Druyvesteyn in 1930, introduced in practice in the fifties, and remains the only technique for experimental study of the EEDF in gas discharge plasmas. Progress in analog and digital electronics has made it feasible to perform an EEDF measurement in any modern plasma experiment where a classical Langmuir probe can be used.

---

*Present Address:
GTE Laboratories, Inc.
40 Sylvan Road
Waltham, MA, 02254 USA

This lecture is an overview of known approaches towards probe measurement of the EEDF in gas discharge plasmas. Such plasmas are encountered in basic research experiments, in light source technology, and in plasma processing devices. Plasma parameters in these areas are typically: plasma densities of $10^8$–$10^{12}$ $cm^{-3}$, mean electron energies of 1–10 eV, and gas pressures up to a few Torr.

## 2. LANGMUIR PROBE METHOD

The plasma probe, introduced by Langmuir more than 60 years ago, gave birth to a new discipline - Plasma Physics. Since that time, the plasma probe has become the most powerful, most developed, and most sophisticated tool for plasma diagnostics.

The ability to deduce the local values of macroscopic plasma parameters (electron temperature, plasma density and plasma potential), as well as to establish electron energy distribution functions just from a measurement of the probe current/voltage characteristics, makes it very attractive in experiments with low temperature plasmas. A great deal of experience in plasma-probe theory and techniques has been gained since Langmuir's time, mainly due to basic research in gas discharge physics and light source technology. These have been summarized in many monographs and reviews.

The task in plasma-probe theory boils down to the problem of coupling probe I/V characteristics, which depend on the plasma perturbation caused by the probe, with the unperturbed plasma parameters in the absence of the probe or far away from it . The probe perturbation, caused by the potential difference between probe and plasma and by the sink of electrons and ions at the probe, is localized around it, forming the probe sheath and pre-sheath. The thickness of this zone is of the order of a few Debye lengths $\lambda_D$.

The usual way of obtaining a probe I/V characteristic is to measure an electric current on a small wire immersed in the plasma and biased by a variable voltage source referenced to a discharge electrode (anode or cathode). This is shown in Fig. 1. Three regions can be distinguished on the typical probe characteristics, which are shown in Fig. 2.

The first one refers to the ion "saturation" current and corresponds to a highly negative probe potential $V_p$. In this region practically all electrons are repelled, and only positive ions are attracted and collected by the probe. The second region refers to an "intermediate" region in which some electrons are repelled, and ions are still accelerated to the probe. The third region refers to the electron "saturation" current and corresponds to a positive probe relative to the plasma potential. In this region ions are fully repelled and electrons are attracted and collected by the probe.

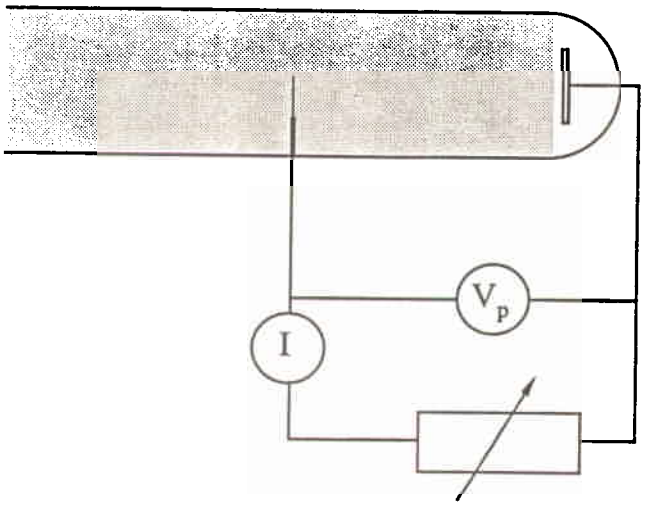


Fig. 1. Typical probe measuring circuit.

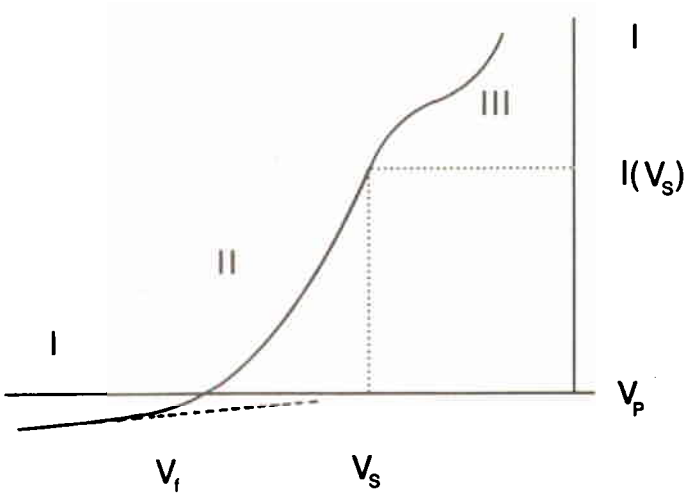


Fig. 2. Typical probe I/V characteristic

These three regions are divided by two characteristic break- points: One of them is easily found as the floating potential $V_f$ where the probe current crosses zero. Here the electron and ion currents are equal. The second point corresponds to plasma potential $V_S$, where the plasma and probe potentials are equal. The position of the plasma potential on the probe (I/V) curve can more easily be seen on a semi-logarithmic plot than on a linear plot as shown in Fig. 3.

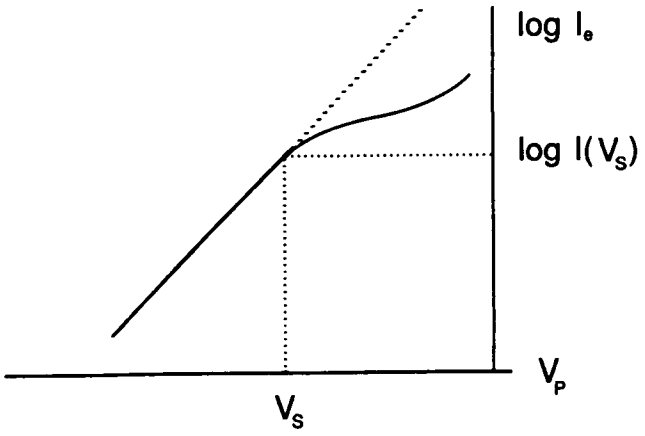


Fig. 3. Semi-log plot of the electron probe current

All three regions of the probe I/V curve carry information about plasma parameters and can be used to extract this information through appropriate processing of the corresponding part of the probe characteristic. However, the point is that each of these three regions has, in essence, a different level of universality, credibility, and manageability when used to obtain plasma parameters. To clarify this, let us consider the simplest case of a small probe with radius a immersed in low pressure plasma. This situation corresponds to a classical Langmuir probe and implies the absence of electron and ion collisions with gas molecules within the probe sheath, and a negligibly small effect on the ionization and energy balance of the plasma due to electron and ion currents drawn to the probe. Note that these requirements can be fulfilled only for small spherical and cylindrical probes, providing the following conditions apply:

$$a \ll \lambda_e \; ; \; \lambda_D \ll \lambda_e \text{ and } \lambda_D \ll \lambda_+$$

where $\lambda_e$ and $\lambda_+$ are the electron and ion mean free paths.

Furthermore, when we discuss plasma probes, we shall assume the collisionless regime, for which these inequalities are satisfied unless otherwise stated.

There are well-developed collisionless theories for spherical and cylindrical probes covering all three regions of the probe characteristic. See, for example, Chung, Talbot and Touryan's book,8. These theories imply Maxwellian distributions for electrons and ions and represent probe I/V characteristics as follows:

$$I = I_e - I_+$$

$$I_e = Aen \left( \frac{kT_e}{2\pi m} \right)^{1/2} \exp \left( \frac{eV}{kT_e} \right) \qquad V<0$$

$$I_e = Aen \left( \frac{kT_e}{2\pi m} \right)^{1/2} \Phi_e \left( V, \frac{a}{\lambda_D}, \frac{T_+}{T_e} \right) \qquad V>0$$

$$I_+ = Aen \left( \frac{kT_+}{2\pi M} \right)^{1/2} \exp \left( \frac{-eV}{kT_+} \right) \qquad V>0$$

$$I_+ = Aen \left( \frac{kT_+}{2\pi M} \right)^{1/2} \Phi_+ \left( V, \frac{a}{\lambda_D}, \frac{T_+}{T_e} \right) \qquad V<0$$

Here, $I_e$ and $I_+$ are the electron and ion probe currents respectively. A is the collection probe area, e is the electron and ion charge, $T_e$ and $T_+$ are the electron and ion temperatures, k is Boltzman's constant, m and M are the electron and ion masses respectively. Here, n is the plasma density, $V = V_p - V_s$ is the probe potential referenced to the plasma potential, and $\Phi_e$ and $\Phi_+$ are functions describing the probe current for attracted particles (i.e. electrons for $V>0$ and ions for $V<0$). $\Phi_e$ and $\Phi_+$ are rather complicated functions of probe voltage and can be expressed analytically only for extreme cases of radial motion when $a >> \lambda_D$ and orbital motion when $a << \lambda_D$. Note that these functions are different for spherical and cylindrical probes and, therefore, can be an additional source of uncertainty in interpreting data obtained with limited cylindrical or partly spherical probes. For example, at high enough negative probe voltage, the sheath surrounding a finite length cylindrical probe has the shape of an ellipsoid rather than that of a limited cylinder and, in order to obtain meaningful values of plasma parameters, a two-dimensional probe theory is needed. But even in the simplest of cases, namely a $>> \lambda_D$ or a $<< \lambda_D$, for which analytical formulas exist and could be applicable to limited cylindrical or non-perfect spherical probes, prior knowledge of the ratio $T_+/T_e$, and the successive iterative techniques are needed to establish plasma parameters from ion or electron saturation curves.

Inferring the plasma parameters from the intermediate region II has definite advantages which make this technique of plasma probe diagnostic so widely used. The most important advantages are detailed as follows:

i) The analytical expression for electron current which is deduced from first principles (Liouville's theorem), does not

depend on the ratios $a/\lambda_D$, and $T_+/T_e$, nor on the shape of the collecting surface (provided it is not concave).

ii) There is a straightforward procedure to obtain the plasma parameters without the need of an iterative technique. For a considerable portion of region II, the electron component of the probe current $I_e$ is greater than the ion current $I_+$. This permits extraction of the electron component $I_e(V_p)$ using a coarse approximation of the ion component $I_+(V_p)$ as it is shown in Fig. 2. When plotted on a semilog scale, the electron part of the probe I/V characteristics, $I_e(V_p)$, gives the electron temperature $T_e$

$$T_e = \frac{e}{k}\left[\frac{d}{dV_p} \ln I_e(V_p)\right]^{-1}$$

and the absolute value of the plasma potential $V_s$, at the point where the function $\ln I_e(V_p)$ declines from being linear, as is seen in Fig. 3.

The value of the total current when $V_p = V_s$ is equal to the electron saturation current $I_e(V_s)$ which is used to find the plasma density

$$n = \frac{I(V_s)}{eA}\left(\frac{2\pi m}{kT_e}\right)^{1/2}$$

Expressions for $T_e$ and n are working formulas of the well-known Langmuir probe method.

iii) The most remarkable feature of the probe I/V characteristic in the intermediate region is that it carries information about the electron energy distribution function (EEDF). This property of the probe I/V characteristic has been used over the last thirty years for probe measurements of the EEDF in gas-discharge plasmas, and this method still remains as the only way of obtaining meaningful experimental data on the EEDF.

For any isotropic EEDF, the electron probe current $I_e$ is related to the EEDF in the undisturbed plasma by the following expression:

$$I_e = \frac{eA}{2\sqrt{2m}} \int_{-eV}^{\infty} (\varepsilon + eV)\varepsilon^{-1/2} F(\varepsilon)\, d\varepsilon \quad , \qquad V<0$$

where $\varepsilon = mv^2/2$ is the electron energy and $F(\varepsilon)$ is normalized as

$$n = \int_0^\infty F(\varepsilon)d\varepsilon$$

In this definition, $F(\varepsilon)$ is the electron density in the energy range $\varepsilon$ to $\varepsilon + d\varepsilon$, or $F(\varepsilon) = dn/d\varepsilon$. Note that different authors use different definitions for EEDF depending on their means of normalization.

$F(\varepsilon)$ can be converted to the electron velocity distribution function (EVDF), $F_v(\varepsilon)$, through the relation

$$F(\varepsilon)d\varepsilon = 4\pi v^2 F_v(\varepsilon)dv$$

For a Maxwellian distribution, the EEDF is

$$F_M(\varepsilon) = \frac{2}{\sqrt{\pi}} n(kT_e)^{-3/2} \varepsilon^{1/2} \exp\left(\frac{-\varepsilon}{kT_e}\right)$$

Differentiation of expression for the electron current gives the well known Druyvesteyn formula,10, which is the basis for EEDF measurements.

$$F(\varepsilon) = \frac{4}{e^2 A}\left(\frac{-mV}{2e}\right)^{1/2} \frac{d^2 I}{dV^2}, \qquad \begin{matrix}\varepsilon=-eV \\ V<0\end{matrix}$$

Two points are worth mentioning here, and they refer to the application of the Druyvesteyn formula:

The second derivative of the ion current $I_+$ is usually much smaller than $I_e''$ unless the negative probe voltage V is too high. Thus, the second derivative of the electron current actually coincides with the second derivative of the total probe current. Effects of the $I_+''$ will be considered separately later.

The second point is the use of the Druyvesteyn formula for diagnostics in electrical discharge plasmas. Indeed, by definition, plasmas with a finite discharge current are always nonisotropic and even a "currentless" bounded plasma cannot be isotropic due to diffusion to the boundaries. Under these conditions, "isotropic EEDF" as referred to the application of the Druyvesteyn formula should be considered only relatively implying just a slight nonisotropic EEDF. By intuition, one can consider the EEDF to be relatively isotropic, providing that the electron drift velocity is much smaller than the thermal one. This is actually satisfied in the majority of cases of gas discharge plasmas. The issue of EEDF measurement in a nonisotropic plasma will be considered in more detail later in this review.

## 3. THE MEASUREMENT OF EEDF

### 3.1 Specific requirement for EEDF measurement

Prior to discussing different methods for determining the second derivative of the probe I/V characteristic, let us specify the main problem encountered in such an undertaking. The problem boils down to the ability to accurately measure and process the second derivative with appropriate energy resolution and signal-to-noise ratio (S/N). Gas-discharge plasmas in themselves are sources of significant noise, which usually originates at the discharge electrodes and/or within the plasma volume. Thus, the probe current is intrinsically noisy. Furthermore, the procedure of differentiation (in the time domain or in the voltage domain) considerably increases the level of high frequency noise (while the opposite procedure of integration reduces it). The S/N ratio of the second derivative measurement determines its dynamic range and the possibility of analyzing the high energy tail of the EEDF. For example, a dynamic range of about 60 db or more is required to analyze high-energy electrons performing ionization. Such a high dynamic range can be achieved only through the use of special filtering and averaging techniques.

A number of arrangements have been developed for obtaining the differentiated probe characteristics and some of them have been described by Swift and Schwar,6, Cherrington,9 and Milenin and Timofeer,11. Here we discuss two basic well-developed and widely-used approaches, each having certain advantages and disadvantages.

### 3.2 AC Measuring Technique

The most popular way of obtaining the second derivative is to use the nonlinear property of the probe I/V characteristic. This is typically done by applying a small ac voltage $\delta(t)$ to the dc biased probe and subsequently measuring some of the filtered components of the probe current which are proportional to its second derivative. These components can

be found in a representation of the probe current by a Taylor's expansion about the probe's dc potential $V_o$,

$$I(V) = I[V_o + \vartheta(t)] = I(V_o) + \vartheta(t)\,\frac{dI(V_o)}{dV} + \frac{1}{2}\,[\vartheta(t)]^2\,\frac{d^2I(V_o)}{dV^2} +$$

As one can see, the term which contains $d^2I/dV^2$ is proportional to the square of the applied ac voltage. This is the origin of those frequency components of the probe current which do not contain the applied ac voltage $\delta(t)$. This permits them to be separated easily from the frequency components of the applied voltage. Depending on the kind of applied ac voltage $\delta(t)$, a frequency component $\Delta^2I(t)$ proportional to $d^2I/dV^2$ can be measured as either a second harmonic or an envelope, or a beat frequency signal. For all these cases, $\Delta^2I(t)$ can be expressed by the formula

$$\Delta^2I(t) \sim B(t)\,\frac{d^2I}{dV^2}$$

where the function B(t), has a form corresponding to each of the input voltages $\delta(t)$ given in the table below.

| Input signal $\delta(t)$ | Result of the nonlinear process | Temporal function B(t) |
|---|---|---|
| $\delta_o \mathrm{Sin}\omega t$ | Second harmonic | $\frac{1}{4}\delta_0^2\ \mathrm{Cos}2\omega t$ |
| $\frac{1}{2}\delta_o(1+\mathrm{Cos}\omega t)\mathrm{Sin}\omega t$ | Demodulation | $\frac{1}{8}\delta_0^2\ \mathrm{Cos}\omega t$ |
| $\frac{1}{2}\delta_o(\mathrm{Sin}\omega_1 t + \mathrm{Sin}\omega_2 t)$ | Beating mode | $\frac{1}{4}\delta_0^2\ \mathrm{Cos}(\omega_1-\omega_2)t$ |

In all these cases the peak value of the applied ac-voltage $\delta_o$ must be small compared with the mean electron energy $\bar{\varepsilon}=3kT_e/2$, otherwise higher order derivatives would contribute to the frequency components of the probe current. On the other hand, the output signal is proportional to $\delta_o$, and therefore it is desirable to have $\delta_o$ large enough to achieve a large S/N ratio. The values of $\delta_o$ which provide an acceptable compromise between the S/N ratio and measurement distortions are usually within an interval of $e\delta_o = (0.1\text{-}0.3)\bar{\varepsilon}$. As one can see in the table, the method which uses

double modulation of the probe voltage has half the sensitivity and is therefore noisier than the other two. On the other hand, it has the advantage of not being as sensitive to circuitry nonlinearities, making it more practical.

A lock-in amplifier which performs functions of filtering, phase sensitive detection, and noise integration, is an integral part of any modification of the ac measuring technique. The lock-in amplifier tremendously increases the S/N ratio. Such enhancement in the S/N ratio is achieved at the expense of slowing the processing speed due to averaging time. This disavdantage of the lock-in amplifier implies point-by-point measurements or a relatively slow record of the output signal.

The ac-measuring technique was first proposed by Sloan and McGregor,12 who measured a dc shift in the probe current. Note that $[\delta(t)]^2$ also has a dc component. But the real practical application of this technique started with Kagan, Malyshev and Fedorov,13,14, Boyd and Twiddy,15 and Branner, Friar and Medicus,16. The most recent detailed description and analysis of this technique is given by Milenin and Timofeev,11 and Schoenberg,17. Some examples of their implementation of the ac-measurement technique together with typical results are given in Figs. 4, 5 and 6.

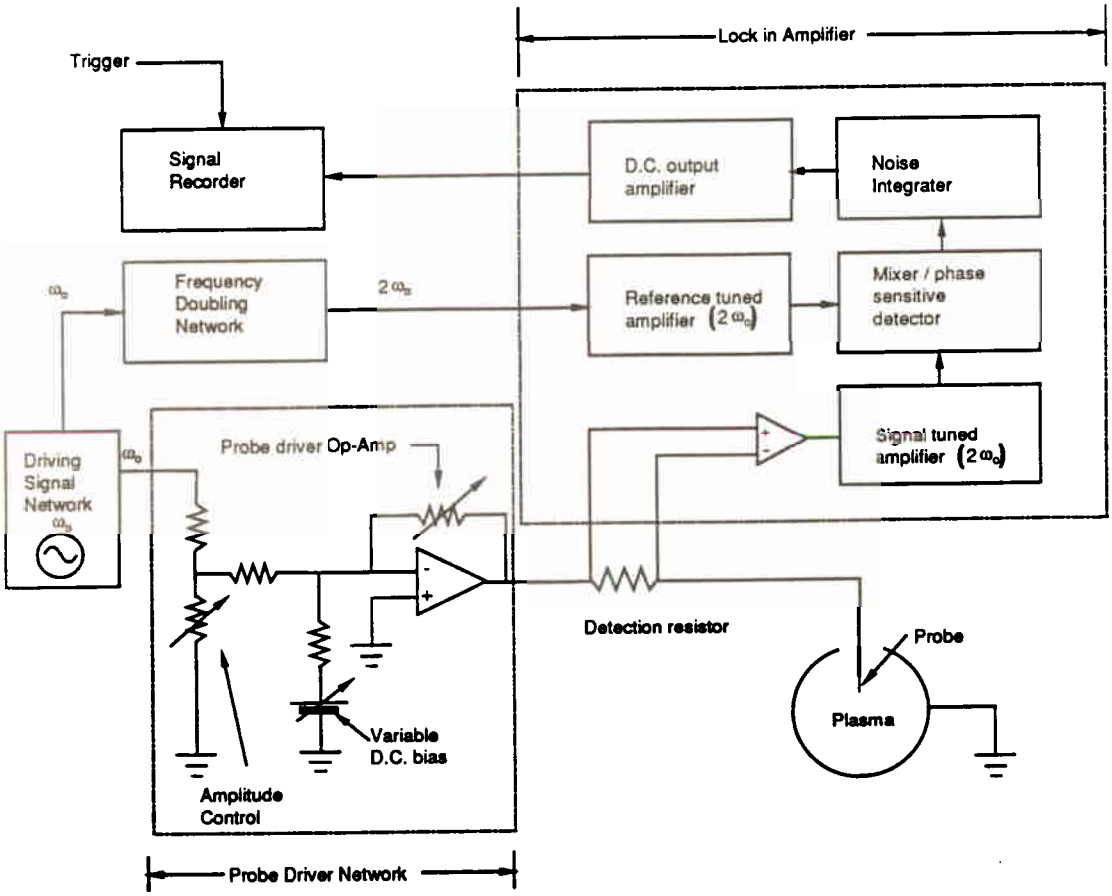


Fig. 4. Second harmonic detection network (after Schoenberg,17)

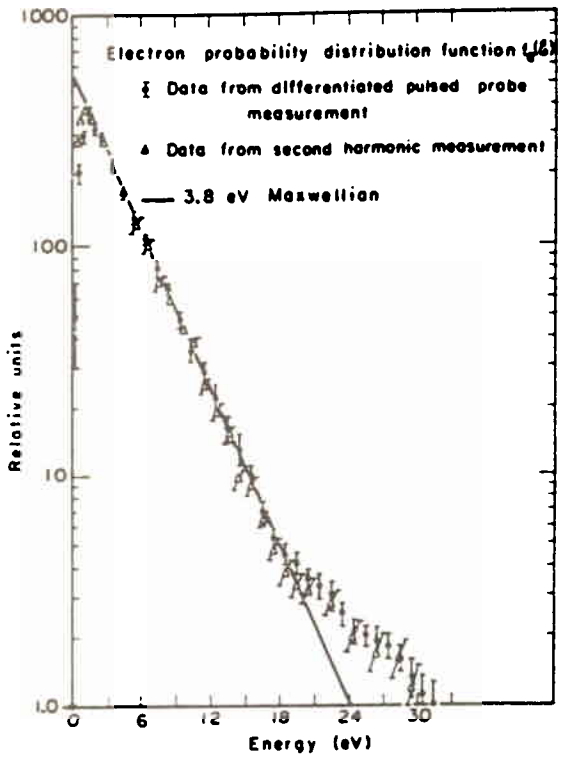


Fig. 5. Second derivative data obtained in Lawrence Berkley Laboratory neutral beam ion source (after Scohenberg,17).

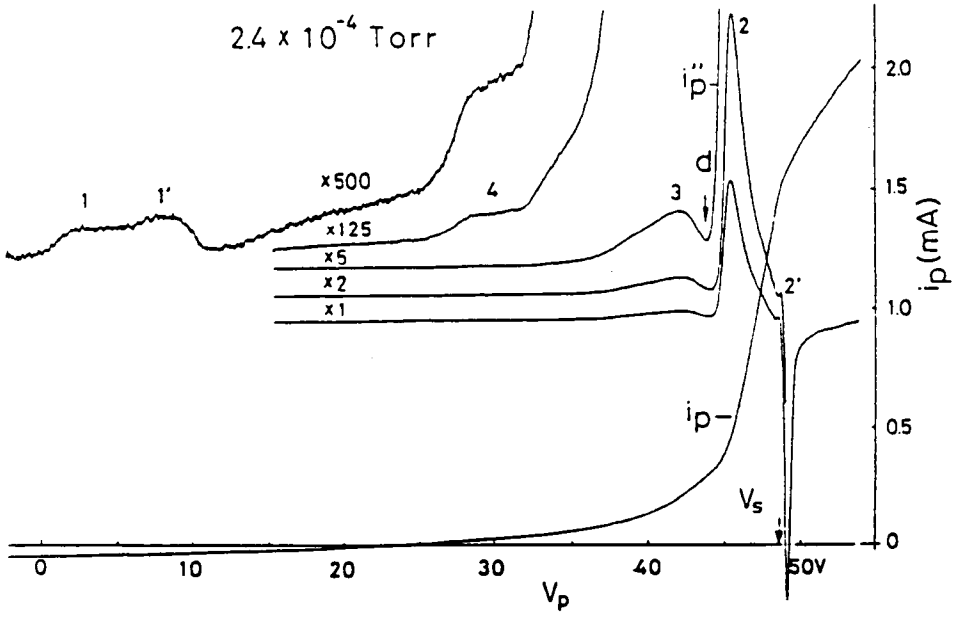


FIG. 6. An example of the probe characteristic and second derivative in a nitrogen plasma of the multiple plasma device; heating mode method adapted from Amemiya (after Amemiya,70).

Note here that displaying the second derivative or probability distribution function on a semi-logarithmic scale, as it is shown in Fig. 5, is more informative than displaying the already processed $F(\varepsilon)$ on a linear scale. The reason for this is the larger dynamic range covered on a semilog scale which allows one to easily see the difference between the experimental EEDF and the Maxwellian distribution function, which looks like a straight line. The direct display of the second derivative can also demonstrate the quality of the experiment. Large energy gaps between zero and maximum (comparable to or more than the mean electron energy) usually reflect some problems, and indicate that the experimental results are questionable.

### 3.3 Pulse measuring technique

The pulse measuring technique is widely used to display Langmuir probe characteristics on an oscilloscope. In this procedure, the voltage applied to the probe is swept linearly in time for short duration. Under these conditions, the second derivative of the probe current in the voltage domain is proportional to that in the time domain, i.e.,

$$\frac{d^2I}{dV^2} = \frac{d^2I}{dt^2}\left(\frac{dV}{dt}\right)^{-2} = \alpha^{-2}\,\frac{d^2I}{dt^2}$$

But attempts at direct differentiation of the probe current in the time domain do not give satisfactory results.

This is easy to understand, since double differentiation in the time domain is equivalent to amplification with the amplifier gain being proportional to the square of the frequency. Thus, the high frequency components of the input noise will literally jam the information-carrying signal. In the application of plasma probes, this problem was considered by Alexeff and Howell,18 and Wiesemann,19. They showed that operational amplifiers can be successfully used for differentiation of the probe current provided the bandwidth of the system is limited. The limitation in bandwidth is required to cut-off the high frequency components of the noise. This concept is illustrated in Fig. 7.

Additional elements $R_2$ and $C_2$ are introduced in a standard differentiating circuit to limit its bandwidth. This

limitation in the bandwidth leads to the deterioration of the temporal, and consequently of the energy resolution of the pulse method. The energy resolution of a differentiator $\Delta\varepsilon$ with a cutoff frequency $f_c$ can be estimated by the following formula,20.

$$\Delta\varepsilon = \frac{e\alpha}{2f_c}$$

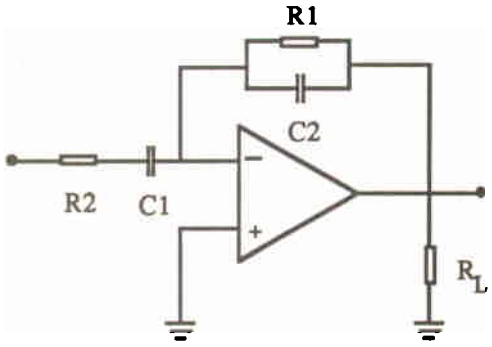


Fig. 7. Bandwidth limited differentiating network.

Again, as in the previously discussed ac technique, there is a tradeoff between the requirement of high energy resolution and high S/N ratio or dynamic range of the measured EEDF.

Examples of the realization of the pulse measuring technique have been described by Nordlund and Breaux,21 and Schoenberg,20. A block diagram of a real-time differentiator together with a real-time EEDF processing device is shown in Fig. 8.

This system allows the fast direct display of log $d^2I/dV^2$ and EEDF as well as plasma parameters n and $T_e$.

A system similar to a previously described system for pulse EEDF measurements has been developed by Schoenberg, 20 with a significant improvement in the dynamic range. This has been achieved by using signal digitizers with the ability to ensemble average over several data sets. The ensemble averaging procedure allows an increase in the S/N ratio by a factor of $K^{1/2}$, where K is the number of sweeps, provided that the noise is random.

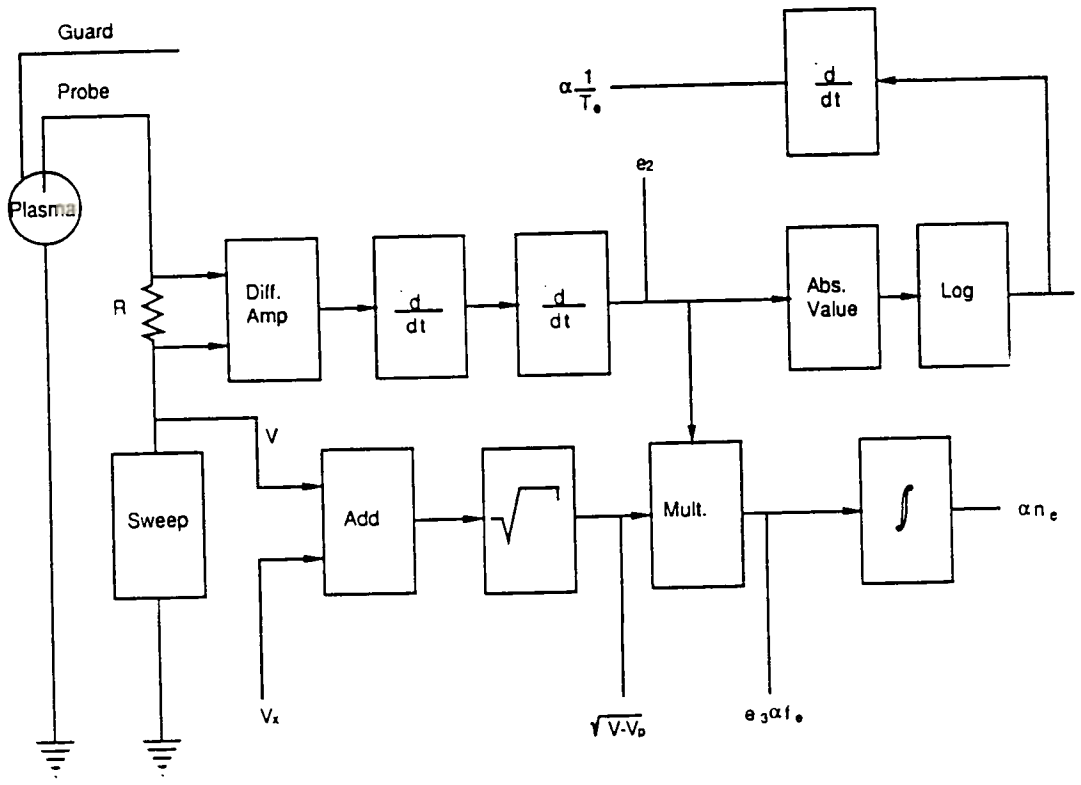


Fig. 8. Block diagram of an analog plasma diagnostic system (after Nordlund and Breaux,21).

Using a pulse technique with differentiating networks has the advantages of fast data acquisition, processing, and display, using available digital oscilloscopes or waveform analyzers. This allows one to measure EEDF's in transient or noisy plasmas providing that the condition for probe sweep time $\tau_\alpha$ satisfies the inequality

$$\tau_\alpha << \tau_p \text{ and/or } f_n^{-1}$$

where $\tau_p$ and $f_n$ are the plasma transient time and the noise frequency bandwidth, respectively.

Other advantages of the pulse-sweep technique are that it does not perturb the plasma-probe sheath and that it provides for the more accurate absolute measurement of the EEDF. In general, the pulse measuring technique appears to be inferior to the ac measuring technique in sensitivity and in dynamic range, and can be used only in rather quiescent plasmas.

An example of the pulse-measuring technique with fully computerized data processing has been given by Hopkins and Graham,22,23. In their system, the second derivative has been obtained from the ensemble-averaged I/V probe characteristic. Central point smoothing (filtering) using a sliding least-squares fit to a second-order polynomial was used to smooth the first derivative of the probe current. The second derivative at the central point was obtained by differentiating the fitted polynomial. Using this technique, these authors studied the discharge current dependence and spatial variations of the EEDF in a magnetic-multipole plasma. Examples of their results are given in Figs. 9 and 10.

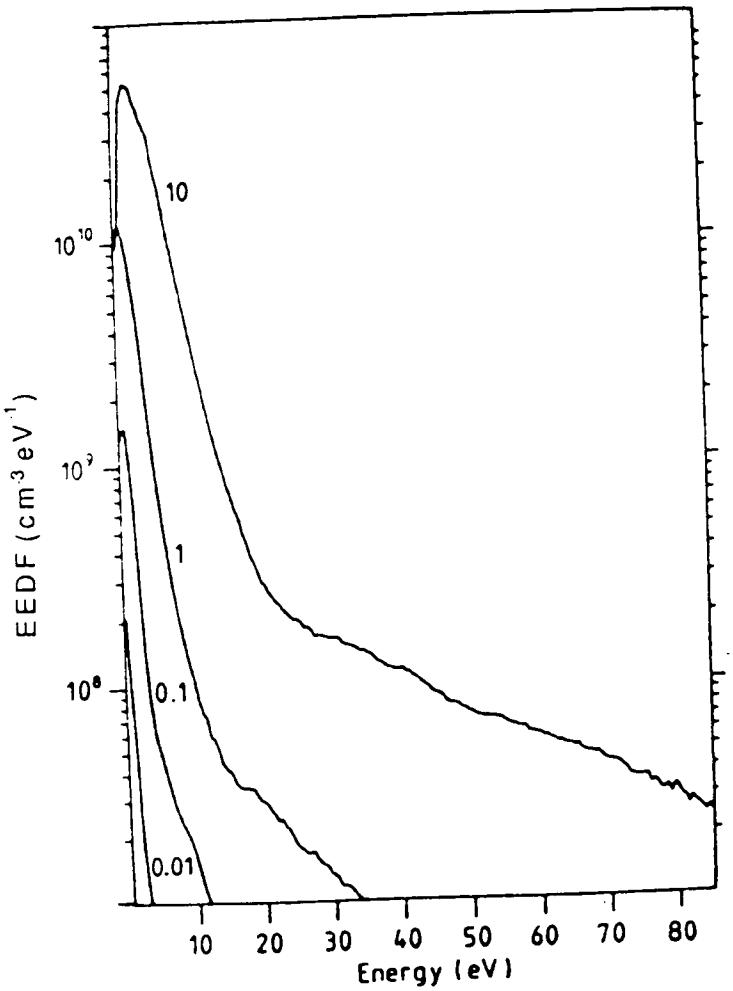


Fig. 9. The variation of the EEDF with discharge current (in amps, against curves) multiple plasma device, hydrogen discharge, p=2mTorr (after Hopkins and Graham,22).

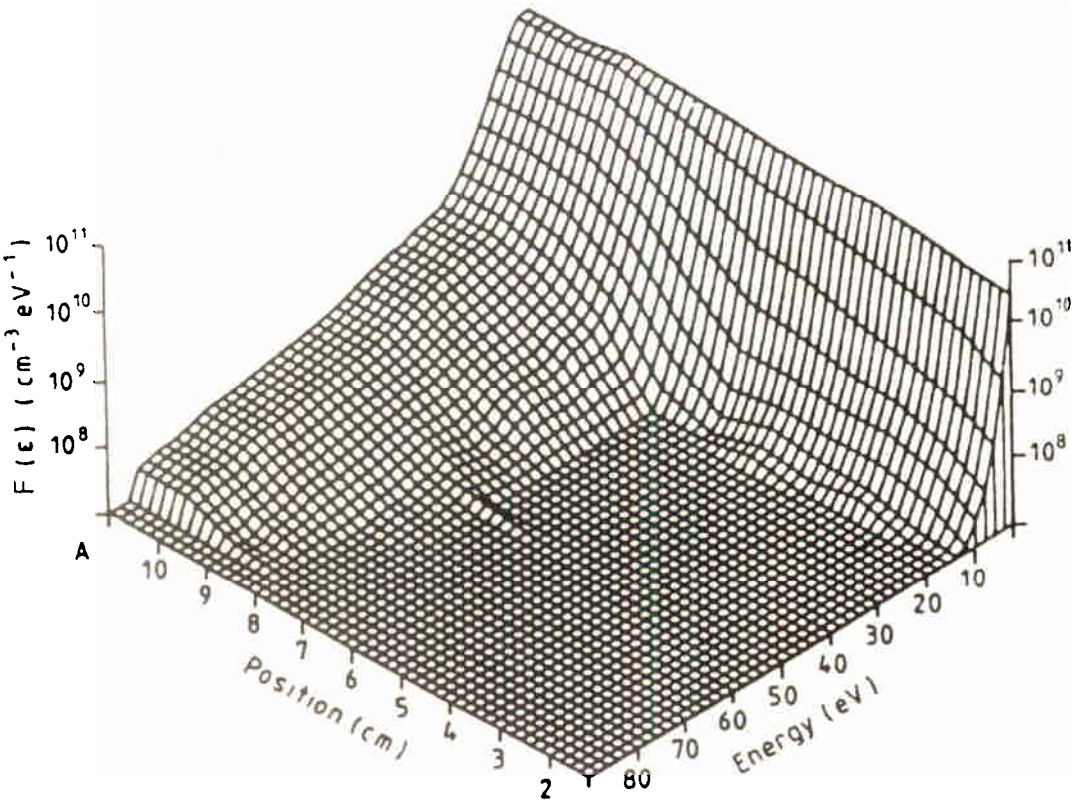


Fig. 10. The spatial variation of the EEDF in multiple plasma device, hydrogen discharge, p=2m Torr (after Hopkins and Graham,22).

## 3.4 Time resolved measurement of EEDF

There are two approaches to the measurement of the EEDF in unsteady plasmas. One of them, already mentioned, is based on fast measurement of the second derivative for a time which is much smaller than that for plasma transients. The second approach, which can be applied only to periodically varying plasmas, is the sampling or gating technique. This technique has been developed for EEDF measurements in self-excited, moving striations by Rayment and Twiddy,24 using the ac method for the differentiation of probe characteristics followed up by numerical differentiation. Different techniques have evolved for EEDF measurements in striations by Oreshak, Stepanov and Stepanov,25 using a pulse technique with

differentiating networks. More sophisticated systems with pulse-biased probes have been developed by Rayment and Twiddy,25 for measurements in high current dc discharges (to prevent the probe from overheating), and by Milenin and Timofeev, 11 for measurement in ac (several kHz) and in pulse-modulated discharges (to eliminate the waveform distortion of the plasma oscillations by the probe). In both of these cases an ac method has been used for differentiation of the probe characteristic.

The concept of time-resolved measurements in periodically varying plasmas involves probe signal acquisition only during the short period of the gating time and integration of this information over a great number of plasma transient periods. By changing the time position of the gate reference with respect to the phase of the plasma transient process, one can carry out time-resolved measurements. Time-resolved measurements of EEDF in pulsed Ne-Hg discharges, with a time resolution of 1 $\mu$S has been performed by Adriaansz,27 using the arrangement shown in Fig. 11.

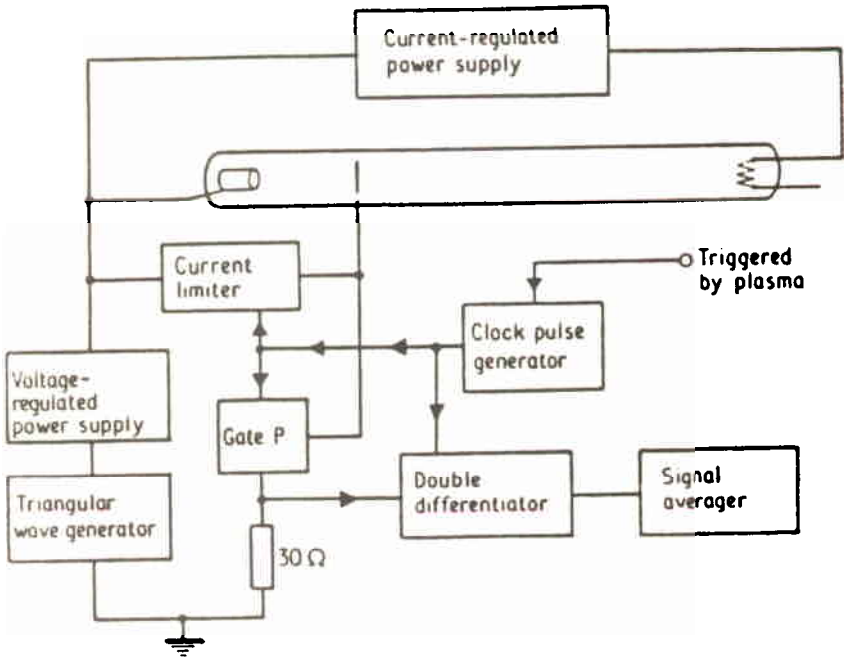


Fig. 11. Block diagram of a plasma diagnostic system with probe gating (after Adriaansz,27).

In this circuit, the probe is connected to ground via gate P and the 30 Ω measuring resistor. Gate P also protects the probe from being damaged by high probe currents caused by the high plasma potential variations in modulated discharge. The clock pulse generator is triggered synchronously with the plasma modulation process and has an adjustable delay, so that

the whole plasma transient period can be scanned. The probe potential is swept with respect to the anode potential by means of a triangular wave generator and biased by a voltage source. A box-car averager is used to increase the S/N ratio and to smooth the signal from the differentiating circuit. An alternate approach has been used here for double differentiation. This actually comprises a second difference of three successive measurements of the probe current

$$\frac{d^2I}{dV^2} \sim I(V-\Delta V) + I(V+\Delta V) - 2I(V) \qquad \text{at } \Delta V \to 0$$

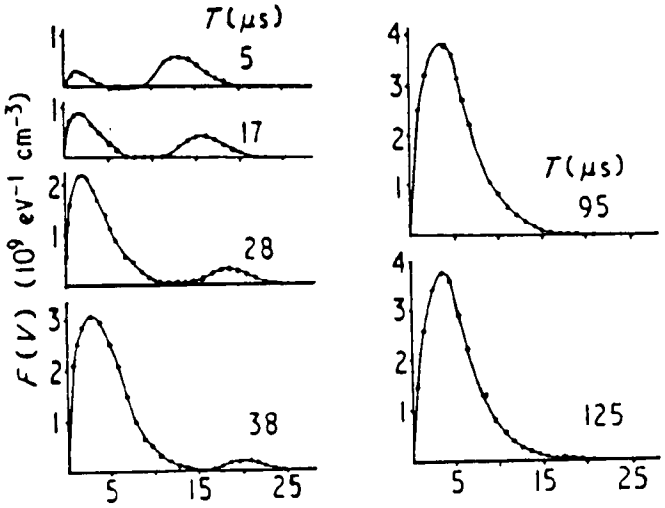


Fig. 12. Series of EEDF measurements through moving striation, neon discharge, p=0.32 Torr (after Rayment and Twiddy,24).

For a probe voltage scanning linearly in time, the successive values of the discharge current can be obtained using time delay circuits. The second-difference technique for the differentiation probe characteristics has also been used by Schimizu and Amemia,28. Examples of the EEDF obtained in periodically varying plasmas are given in Fig. 12.

## 4. PROBE DIAGNOSTICS OF ANISOTROPIC PLASMAS

There are several situations where one can expect a strong anisotropy in the EEDF. These are: plasmas in magnetic fields, low pressure gas discharges at very high E/P, when the electron drift velocity approaches a thermal one, cathode glow plasmas and RF plasmas maintained by fast cathode or secondary electrons, and plasmas in the presence of a double layer. Generally speaking, the Druyvesteyn formula is not applicable at such conditions, but there are some special cases where one still can use this formula for adequate EEDF measurement.

Kagan and Perel,29 showed that the magnetic field does not affect the I/V probe characteristic for a thin cylindrical probe oriented perpendicular to the magnetic field, if the Larmor radius of the electrons is much greater than the probe radius. It is important that the Larmor radius exceed the probe radius and not the dimensions of the perturbed region or the probe length.

The Druyvesteyn's formula is applicable under these conditions. Using thin cylindrical probes ($a = 20\ \mu$) Vorobjeva, Zaharova and Kagan,30 have measured EEDF in the positive column of the mercury discharge ($p = 1.2{:}10^{-3}$ Torr) and the neon discharge ($p = 2.10^{-2} - 10^{-1}$ Torr) for magnetic fields of up to 800 Oe. They showed that at these conditions, application of the magnetic field reduces the electron temperature and increases the plasma density while the EEDF remains Maxwellian as it is in the absence of the magnetic field.

EEDF behind and in front of the stationary plasma sheath in a low pressure mercury discharge has been measured by Wiesemann,31 and Anderson,32. Note that the Druyvesteyn formula can be applicable for angle averaged measurement of anisotropic EEDF with a small spherical probe providing that the condition of isotropy holds in a perturbed zone around the probe or that the thickness of this zone is much smaller than the probe radius ($\lambda_D << a$). It seems the last condition was the case in Anderson's experiment. More arguments pro and con towards the application of a spherical probe for measurement of an anisotropic EEDF can be found in Allen's note and Anderson's reply,33.

Analyzing the possibility of probe diagnostics on an anisotropic plasma, Lukovnikov,34 showed that for a very simple case when the electron velocity distribution function can be represented by the first approximation solution of the kinetic equation for electrons in an electric field,

$$f_e(\varepsilon,\theta) = f_o(\varepsilon) + f_1(\varepsilon)\cos\theta$$

that only the isotropic part of the distribution contributes to the probe characteristics.

Here $f_o(\varepsilon)$ and $f_1(\varepsilon)\mathrm{CoS}\theta$ are the isotropic and the anisotropic parts of the $f_e(\varepsilon,\theta)$ and $\theta$ is the angle between the direction of the electron velocity and the symmetry axis of the plasma.

The more general analysis of the probe I/V characteristics for axially symmetric plasmas has been given by Fedorov,35, Mezentsev, Mustafaev and Fedorov,36 and Fedorov and Mezentsev,37. They expanded the anisotropic velocity distribution function

$$f(\bar{v}) = \sum_{j=0}^{\infty} f_j(v) P_j(\cos\theta)$$

Here v is the modulus of the electron velocity v and $f_j(v)$ is the expansion coefficient as a function of v. Using this expansion Fedorov,35 has found a relation between the second derivative of the probe current and $f(v)$ for various probe configurations and arbitrary orientations. Particularly, for the cylindrical probe with a >> $\lambda_D$, pointing along and normal to the discharge axis, the second derivatives can be expressed as follows:

$$I''_{\perp} = \frac{2\pi e^3 A}{m^2} \sum_{j=0}^{\infty} \Psi_j(-eV) P_j(0)$$

and

$$I''_{\parallel} = \frac{2\pi e^3 A}{m^2} \sum_{j=0}^{\infty} \Psi_j(-eV) \int_0^{\pi} P_j(\cos\theta)\, d\theta$$

where $\Psi_j$ is the auxiliary function which is expressed in terms of the expansion coefficients $f_j(-eV)$

$$\Psi_j(-eV) = f_j(-eV) - \int_{-eV}^{\infty} f_j(\varepsilon) \frac{\partial}{\partial(-eV)} P_j\left(\sqrt{\frac{eV}{-\varepsilon}}\right) d\varepsilon$$

It follows from these formulas that cylindrical probes can only be used to find the even-index terms in $f_j$ and the number of coefficients $f_j$ that can be determined depends on the number of independent probe orientations. Two probe orientations suffice to find the coefficients $f_0$ and $f_2$, providing that coefficients $f_4$, $f_6$ ... contribute very little to the probe current. In this case, we have

$$f_0(-eV) = \frac{m^2}{6\pi e^3 A} \left(I''_{\perp} + 2I''_{\parallel}\right)$$

$$\Psi_2(-eV) = \frac{2m^2}{3\pi e^3 A} (I''_{\perp} - I''_{\parallel})$$

and the coefficient

$$f_2(-eV) = \Psi_2(-eV) + \frac{3}{2}(-eV)^{-3/2} \int_{-eV}^{\infty} \varepsilon^{1/2} \Psi_2(\varepsilon) d\varepsilon$$

follows by integrating the known function $\Psi_2(-eV)$.

The odd index $f_j$ can be found by solving the kinetic equation. To find $f_j$, they used the kinetic equation in the following form

$$\bar{v}\ \mathrm{grad}_r\left(f_o + \frac{2}{5} f_2\right) + \frac{eE}{m}\left[\frac{\partial f_o}{\partial v} + \frac{2}{5}\frac{1}{v^3}\frac{\partial}{\partial v}\left(v^3 f_2\right)\right] + \nu_{ea} f_1 = 0$$

where $\nu_{ea}$ is the electron-atom collision frequency.

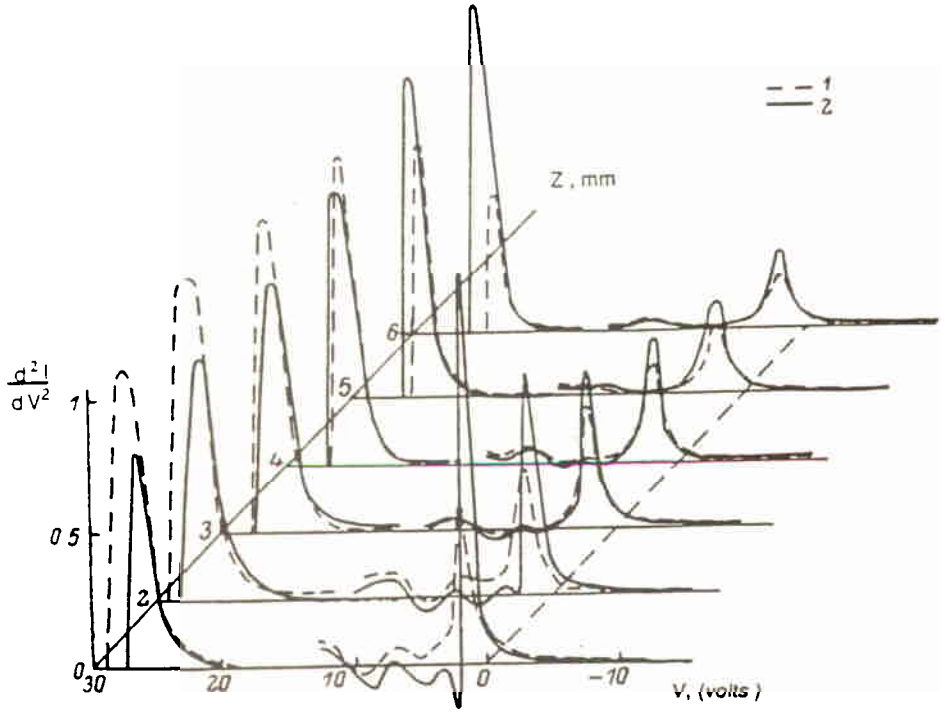


Fig. 13. The second derivative (arbitrary units) at several distances Z from the cathode in the helium arc discharge; p=2.5 Torr, discharge current $I_d$=0.1A, discharge voltage $V_d$=26V. The dashed and solid curves correspond to parallel and perpendicular probe orientation. The high energy part of $d^2I/dV^2$ is shown in X10 scale (after Mezentsev and Mustafaev,38).

The sets of the second derivatives with differently oriented cylindrical probes obtained at the different distance Z from the cathode of the arc discharge are shown in Fig. 13.

The presence of a large group of fast electrons indicates that $f(v)$ is in nonequilibrium, while the negative value of $d^2I/dV^2$ and dependence of $d^2I/dV^2$ on the probe orientation indicates a high degree of anisotropy.

Fig. 14 shows results for $f_o$, $f_1$ and $f_2$.

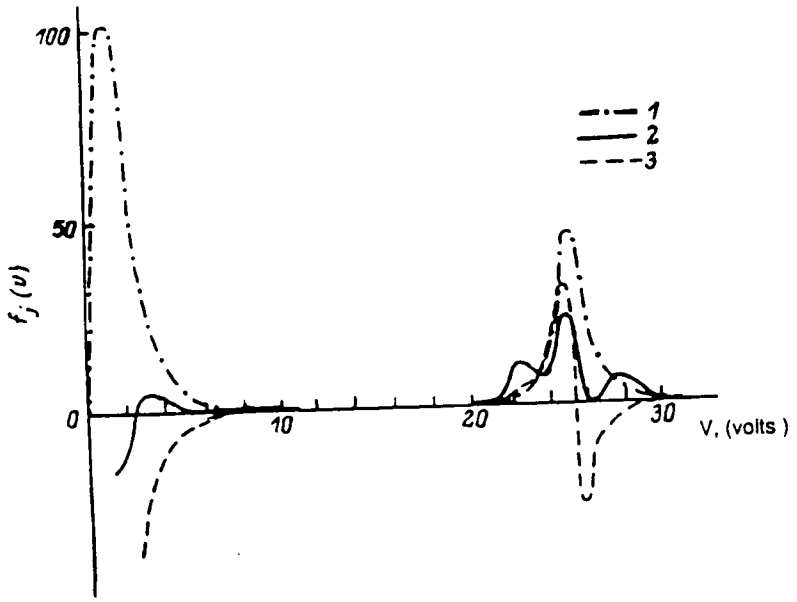


Fig. 14. Expansion coefficients for f(v) (arbitrary units), Z=4mm, 1) $f_o$; 2) $f_1$; 3) $f_2$ (after Mezentsev and Mustafaev,38).
The coefficient $f_1$ can be used for the discharge current $I_d$ calculation

$$I_d = \frac{4\pi}{3} e \int_0^\infty v^3 f_1(v) dv$$

that can be compared with the experiment and thus be a verification of the function $f_1(\varepsilon)$.

The three-term approach for reconstructed EVDF $f(v)$ can be presented as follows:

$$f(\bar{v}) = f_o(v) + f_1(v) \cos\theta + f_2(v) \frac{3\cos^2\theta - 1}{2}$$

## 5. PROBLEMS IN EEDF MEASUREMENTS

### 5.1 Basic requirement for Langmuir probe diagnostics

It has been mentioned by Schott,4 that there is no plasma diagnostics method other than probe diagnostics where the dangers of incorrect measurements and erroneous interpretation of results are so great. It is important to realize that even small errors in the measurement of I/V probe characteristics can result in enormous distortions in the EEDF which is found from the differentiated probe characteristics. Thus it is very important to fulfill the basic requirements of regular plasma-probe diagnostics for accurate measurement of the EEDF.

A number of difficulties in probe measurements have already been pointed out and discussed in numerous text books and reviews on the subject, see for example Cherrington's review,9. Let us enumerate some requirements of correct probe measurement. As has already been mentioned, a probe has to be small to prevent plasma perturbations beyond those which have already been taken into consideration in the probe theory. This implies that the probe radius a is much smaller than the characteristic dimensions of the plasma such as the electron mean free path $\lambda_e$, the ionization length $\lambda_z$, and energy length of relaxation $\lambda_\varepsilon$ and field homogeneity length $\lambda_E = E(\nabla E)^{-1}$. In this respect a large plane probe can be a source of significant plasma perturbations even in a collisionless plasma.

There are at least three kinds of distortions which one can encounter when EEDF is measured with a probe which is not small enough. Two of them are related to hydrodynamic effects on the plasma density depletion around the probe.

When the inequality $a \ll \lambda_e$ is not satisfied, the plasma depletion occurs due to the fact that the electron sink to the probe cannot be fully compensated by electron diffusion. This kind of plasma perturbation was considered by Waymouth,39 (see also 6 and 62), and can lead to a significant distortion of measured EEDF for low energy electrons.

Another kind of plasma perturbation occurs when the inequality $a \ll \lambda_z$ is not satisfied. It is caused by a large probe and occurs even in collisionless plasmas. This kind of plasma perturbation is similar to that which occurs near the dielectric walls confining the plasma, and is a consequence of a change in the ionization balance due to ambipolar plasma flow to the probe. This plasma depletion around the probe, and its holder, has been studied by Cornelissen and Merks-Eppingbroek,40.

Perturbation of the EEDF tail by the probe has been considered by Waymouth,41. This can occur when the sink of high energy electrons to the probe becomes comparable with the rate of their generation due to Coulomb electron-electron interaction. To neglect this effect for Maxwellian electrons

with energy an order higher than the mean energy, the following criterion, based on Waymouth's calculation, has to be satisfied:

$$\frac{n}{A} >> 10^4 \frac{T_e^2}{\lambda_\varepsilon^3}$$

Here n is expressed in $cm^{-3}$; $T_e$- in °K; A- in $cm^2$; $\lambda_\varepsilon$- in cm.

It has been mentioned many times that an insulating probe holder has to have a small enough radius to prevent plasma depletion in the probe vicinity. Note that the wrong design for the probe holder is the most frequent case of a bad probe experiment. Examples of bad and good probe embodiments are given in Fig. 15.

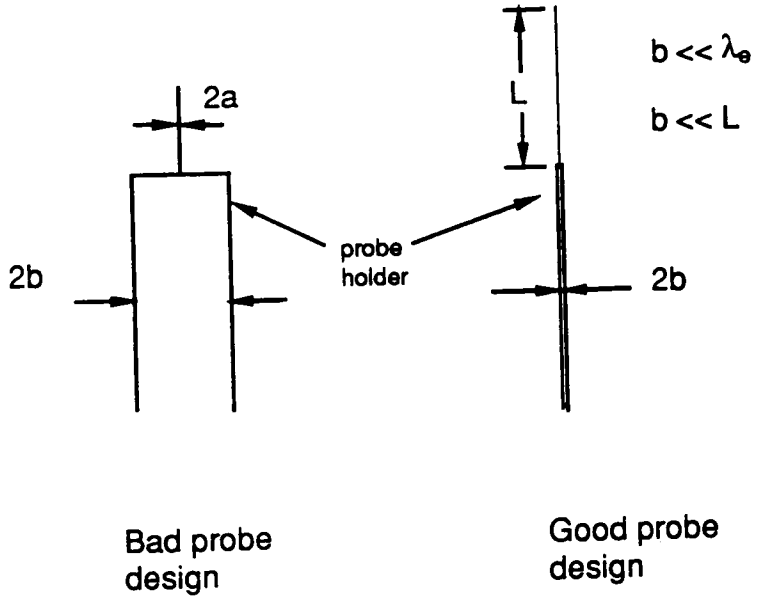


Fig. 15. Examples of a bad and a good probe emodiment.

Serious problems can arise when using probes in chemically reactive plasmas. Probe contamination by plasma constituents can lead to signficiant distortion of the probe characteristics. Plasma noise and oscillations, as well as RF oscillations to the plasma potential in RF excited plasmas, can make the EEDF measurement impossible unless special precautions are undertaken.

Later we will consider typical problems encountered in EEDF measurements in more detail.

## 5.2 Plasma Potential

It is very important to know the plasma potential location on the curve of the second derivative for the proper

calculation of the EEDF. According to classical probe theory, the plasma potential $V_s$ is determined by the inflection point on the I/V characteristic where the second derivative has a discontinuity. This means that the second derivative falls from its maximum to zero when the probe potential equals the plasma space potential. However, in experiments, the maximum and zero locations of the second derivative do not coincide as shown in Fig. 16.

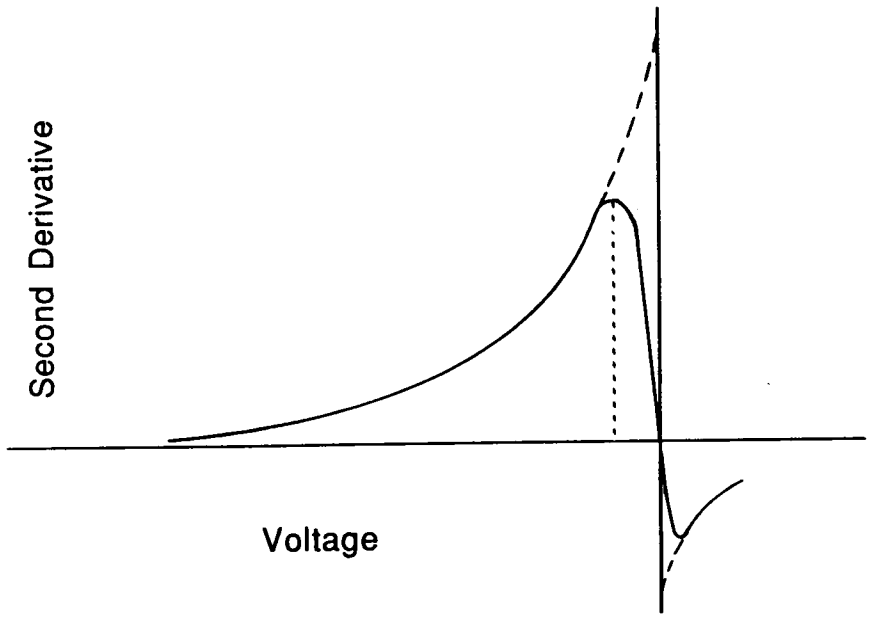


Fig. 16. Second derivatives for ideal and real probes.

The voltage interval between the maximum and zero can sometimes reach several volts, which is a value comparable to or even greater than the mean electron energy. In this case, a considerable error can be expected in calculated EEDF.

The analysis of reasons leading to such a distortion shows that the principal ones are: Probe contamination, which forms a low conductance layer on its surface; finite resistance of the plasma and/or electronic circuit resistance (sensitive resistance and output resistance of the probe ac and dc voltage source); finite amplitude of the ac differentiating voltage in an ac- differentiating method or finite frequency bandwidth of the electronic differentiators; large plasma noise and RF oscillation of the plasma potential referenced to a grounded probe circuit; and, finally, effects of plasma depletion caused by electron sinks on the probe which take place at finite $a/\lambda_e$ ratio. Usually, for a good probe experiment, the gap between the maximum and zero of the second derivative $e\Delta V$ does not exceed $(0.2\text{-}0.3)\bar{\varepsilon}$, otherwise, when $e\Delta V > \bar{\varepsilon}$, some of the above-mentioned problems will probably

take place and one can expect significant distortions in EEDF measurements.

In any case, the question of the reference point for the plasma potential usually arises. This subject has been especially studied by Lukovnikov and Novgorodov,42 who analyzed the results of various investigations and compared them with their own probe measurements of plasma parameters having determined the plasma potential at points where $d^2I/dV^2$ is maximum and zero with the parameters obtained by microwave methods. They conclude that the plasma potential corresponds to the point where $d^2I/dV^2$ crosses zero.

Volkova, Devyatov and Sherif,43 proposed finding the plasma potential using the plots of $\ln[n(V_s^1)]$ and $\bar{\varepsilon}(V_s^1)$, whee $V_s^1$ is an arbitrarily chosen plasma potential, and $n(V_s^1)$ and $\bar{\varepsilon}(V_s^1)$ are found as corresponding integrals of the EEDF. They found that these functions have knees at the point where $V_s^1$ is equal to the true plasma potential. The last occurred at the point where the second derivative crosses zero. Thus, the zero-crossing point should be taken as the plasma potential for calculations of the EEDF. Note that some interpolation of the second derivative to the plasma potential is needed to avoid EEDF's with a hole at low energy electrons. This interpolation can be done exponentially and usually gives a several percent correction in calculations of plasma density n and mean electron energy $\bar{\varepsilon}$, providing that the energy gap between maximum and zero of the second derivative is not too large.

## 5.3 Plasma and circuit resistances

Probe measurement techniques are based on the assumption that a change of applied probe voltage between the probe and some reference electrode is localized in the probe sheath. In other words, the differential resistance of the plasma $R_p$ and an external probe circuit resistance $R_c$ are negligibly small with respect to the minimal differential probe resistance R. The circuit resistance $R_c$ consists of a sensor resistor $R_s$ which is used for the measurement of a signal proportional to the probe current and an output resistance for a probe voltage source $R_o$. Thus the following requirement has to be satisfied for correct probe measurements: $R_p + R_s + R_o = R^1 << R$. The distortion in the second derivative measurement due to finite resistance $R^1$ depends on the technique of differentiating the probe characteristic. For the second harmonic method as shown by Berger and Heisen,44 a signal proportional to the second derivative is reduced by factor $R^3/(R+R^1)^3$. One can see that for small ratio $R^1/R$ the relative error in the second derivative measurement is $3R^1/R$.

The value of minimal differential probe resistance $R = (dI/dV)^{-1}$ at $V_p=V_s$ can easily be found for a Maxwellian approximation of the EEDF, as $R = kT_e/I_e(V_s)$. The use of suitable op-amps allows one to design a probe circuit with very low $R_o$ ($\leq 1\Omega$). However, the plasma differential resistance $R_p$ in some cases may be a serious problem.

In gas discharge plasmas, the value of $R_p$ is negligibly small or even slightly negative for dc, or ac with a frequency lower than the ionization frequency Z, of the discharge plasma (which is of the order of several kilohertz). At frequencies higher than Z, the $R_p$ value can be estimated using the plasma conductivity formula. The tendency of the discharge plasma to be unstable can be a reason for the stimulation of plasma oscillations by ac components of the probe current even in initially quiescent plasmas. Such oscillations along the discharge plasma would have the effect of increased plasma resistance. Thus, for accurate EEDF measurement, the frequency spectrum of the time-varying probe voltage has to be out of the spectrum of possible plasma oscillation modes.

The measurement of EEDF using an ac method performed by Amemiya and Shimizu,45 has demonstrated a frequency dependence in EEDF measurements for frequencies much lower than the plasma frequency. One can explain this result by a frequency dependence of the plasma impedance contributing to the total impedance of the measurement circuit.

## 5.4 Probe contamination

Probe contamination can be a serious problem in regular probe as well as in EEDF measurements. A brief review of this problem has been given by Swift and Schwar,6 and Charrington,9; see also 52, 53 and 89. Probe contamination can create a low conductivity layer on the probe which leads to considerable distortion within the maximum of the second derivative.

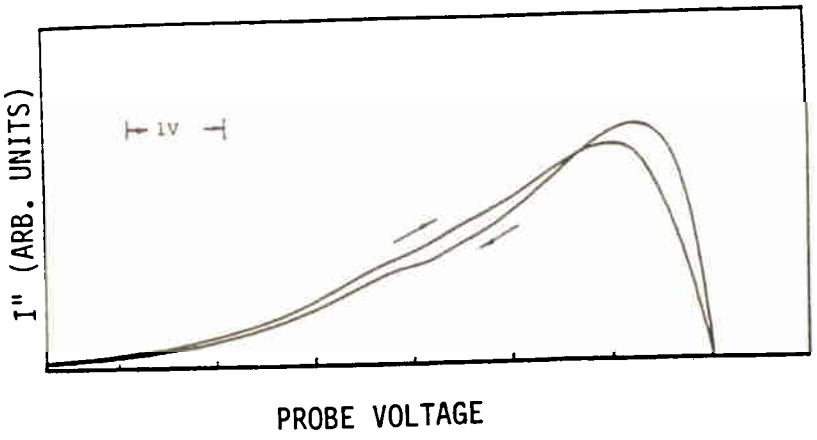


Fig. 17. Hysteresis in a second derivative measurement. Probe voltage rate 0.2V/S. Neon-mercury discharge (author's measurement).

But the most significant problem caused by probe contamination is its influence on the probe work-function 26,46-51. Estimation shows that even at very low levels of residual gases with corresponding gas pressure of $10^{-6}$ Torr, a monolayer appears on the probe for times less than one minute. It has been found that the probe work function is very sensitive to the probe temperature. Change in the probe current due to a slow sweep of the probe voltage causes its temperature to drift and consequently to change its work-function. This results in probe characteristic distortion since the probe sheath voltage under such conditions does not correspond to the applied probe voltage. As has been shown by Rayment and Twiddy,26, the change in the probe work-function could reach 1.5 volts, and there are at least two different time constants (2 and 15 seconds) for this process. The change in the probe work-function during probe measurements can easily be seen in the hysteresis of the probe characteristics obtained for different directions of the probe voltage scanning. This hystereis is shown in Fig. 17 for the second derivative measurement in a neon-mercury discharge.

The hysteresis disappears for very fast probe voltage sweeps when, due to thermal inertia of the probe, its temperature and work-function remain constant during the voltage scanning, or for very slow scanning when probe work function is in equilibrium with probe voltage. It is evident that, in the latter case, the probe characteristics and its second derivative are distorted.

Thus, to eliminate change in probe work-function during probe measurement, one has to scan the probe voltage for a time which is much smaller than the work-function time constant. This can be achieved by using a pulsed probe technique with a probe- scanning time less than or equal to a few ms. To clean the probe between measuring pulses, a large negative (or positive) bias voltage is applied to the probe. For a negative-biased probe, ion bombardment cleans the probe surface, while for a positive- biased probe, electrons heat the probe providing it has a clean surface. Using pulse-probe techniques with negatively biased probes between the pulses, Waymouth,54 managed to perform probe measurement in arc discharge plasmas in the vicinity of an oxide cathode. Later, a similar technique was used in EEDF measurements by many authors,20,21,24. Unfortunately, this in situ technique for probe cleaning cannot be used with the ac differentiation technique since the latter usually requires slow lock-in amplifier averaging.

## 5.5 Application of regularization methods in EEDF measurement

As has already been mentioned, the signal/noise ratio and the dynamic range in EEDF measurements can be improved by increasing the differentiating ac voltage in the ac method or by narrowing the frequency bandwidth of the differentiating circuit in pulse methods. However, these would deteriorate the energy resolution of the measurement which usually

manifests itself in the smoothing of the second derivative near its maximum and in growth of the voltage gap between the maximum and zero of the second derivative. In practice, a maximal level of ac differentiating voltage can be found as that for which the second derivative signal remains proportional to the square of the applied differentiating voltage. The minimal frequency bandwidth in the pulse method can be found as that for which the voltage difference between maximum and zero of the second derivative remains constant.

For a very noisy environment, however, one needs to use a large differentiating voltage to obtain a reasonable dynamic range in EEDF measurement. In this case, there is the possibility to take into account the distortion effect introduced by finite amplitude of the differentiating voltage or introduced by limited frequency bandwidth of the differentiators. This possibility was first demonstrated by Wiesemann,55, see also 56, for ac differentiating method and later was developed for different shapes of differentiating voltage,57 and for differentiating analog circuits,58. Distortion effect in the second derivative measurement can be

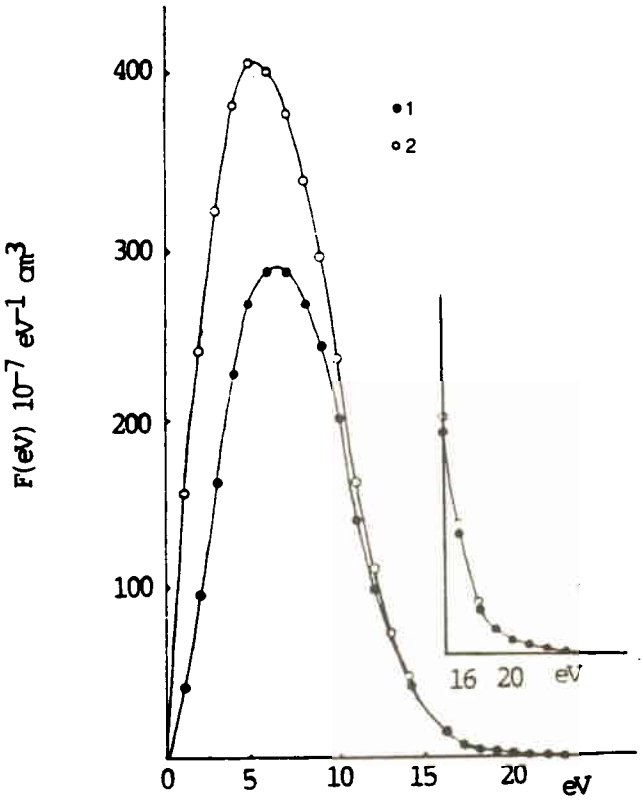


Fig. 18. Influence of the finite rate of electron diffusion on the EEDF measurement. RF discharge in neon, p=5 Torr. 1) Measured EEDF; 2) EEDF incorporating the loss of eletron at the probe (after Vagner and Ignat'ev,63).

taken into account by introducing an instrumental function whose shape can be calculated or separately measured in a special experiment. The instrumental function depends on the method used to take the second derivative. The measured second derivative is the convolution of the true second derivative with the instrumental function. To find the true second derivative one has to deconvolute results of measurements. This procedure reduces to numerically solving (regularization) an integral equation whose kernel is the instrumental function. Deconvolution techniques for improving experimental data in probe measurements have been used by many authors. They have been used for resolution improvement in EEDF measurements on high energy electrons,59 in accounting for effects of electron reflection and secondary emission,60,61 and for correction of the distortion caused by electron sink to the probe at finite ratio $a/\lambda_e$,6,62,63. An example of such improvement in EEDF measurement is shown in Fig. 18 for the condition when distortion was due to finite ratio of $a/\lambda_e$.

It is worth mentioning that the regularization technique has a limited capability for improving experimental data. Because the deconvolution itself is mathematically ill-posed, error accumulation effect does not permit drastic improvement of significantly distorted data.

## 5.6 Influence of ions on the EEDF measurement

It has been shown by Dovzhenko, Ershov and Solntsev,64 that the second derivative of the ion current $I_+''$ can contribute to the second derivative of the total probe current for a highly negative probe voltage. Under such a condition, an error in the determination of the EEDF can be expected in the high energy tail of the EEDF. These authors have calculated the ratios between $I_e''$ and $I_+''$ for radial and orbital motions of ions in the cylindrical probe sheath as a function of the probe voltage assuming a Maxwellian EEDF. They have shown that a signficiant contribution of $I_+''$ to the total second derivative should take place for thin probes with $a/\lambda_D \leq 1$ as well as for light gases. Under these conditions, an orbital motion of ions in the probe sheath takes place and the ratio $I_e''/I_+''$ can be estimated using the following formula:

$$\frac{I_e''}{I_+''} = \left(\frac{4\pi M}{m}\right)^{1/2} \chi^{3/2} \exp(-\chi); \qquad \chi = \frac{-eV}{kT_e}$$

Results of more detailed calculations based on Laframboise's theory,66 have been given by Mosburg,65 for a set of $a/\lambda_D$ ratios from 0 to 100 and for $T_+/T_e$ equal to 0 and 1. The above formula can be used for estimations of the maximum ion influence on the second derivative measurement since for $a>\lambda_D$ and $T_+ \neq 0$, this influence has to be somewhat smaller. The relative values of $I_e''$ and $I_+''$ calculated as functions of $-eV/KT_e$ using this formula are given in Fig. 19.

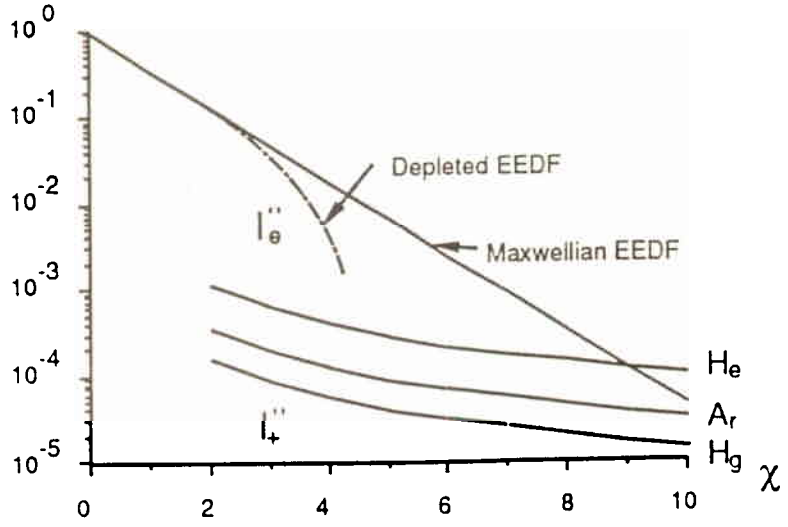


Fig. 19. Ion influence on EEDF mesurement.

As one can see, the ratio $I_+''/I_e''$ depends on the probe voltage and, at a given probe voltage, is somewhat higher for EEDF's having a deficit of high energy electrons. Thus, to avoid the influence of the ion current on EEDF measurements, one should not use very thin probes. There is another possibility: using two probes,67. One of them is thin for measurement near the plasma potential to minimize plasma perturbation by the probe, and the second is thick for measurement at high negative probe voltage to avoid the ion influence on EEDF measurement.

Another kind of ion influence on EEDF measurement can take place in discharges with negative ions,68. The maximum ratio of negative ion current $I_-$ to electron current $I_e$ for a probe at the plasma potential is

$$\frac{I_-}{I_e}\Big|_{V=0} = \frac{n_-}{n_e}\left(\frac{M_- T_e}{mT_-}\right)^{-1/2}$$

which, even for $n_- > n_e$, is very low and cannot affect the I/V probe characteristics. However, the ratio of their second derivatives is $(T_e/T_-)^2$ times larger and for non-isothermal gas discharge plasmas with $T_e >> T_-, T_+$, the influence of negative ions can be large enough to be detected in the second derivative measurement. The effect of negative ions on the probe characteristics has been studied theoretically and experimentally by Amemiya,69. See also 70,71. Examples of

probe characteristics together with their second derivatives obtained in argon-iodine discharges are shown in Fig. 20.

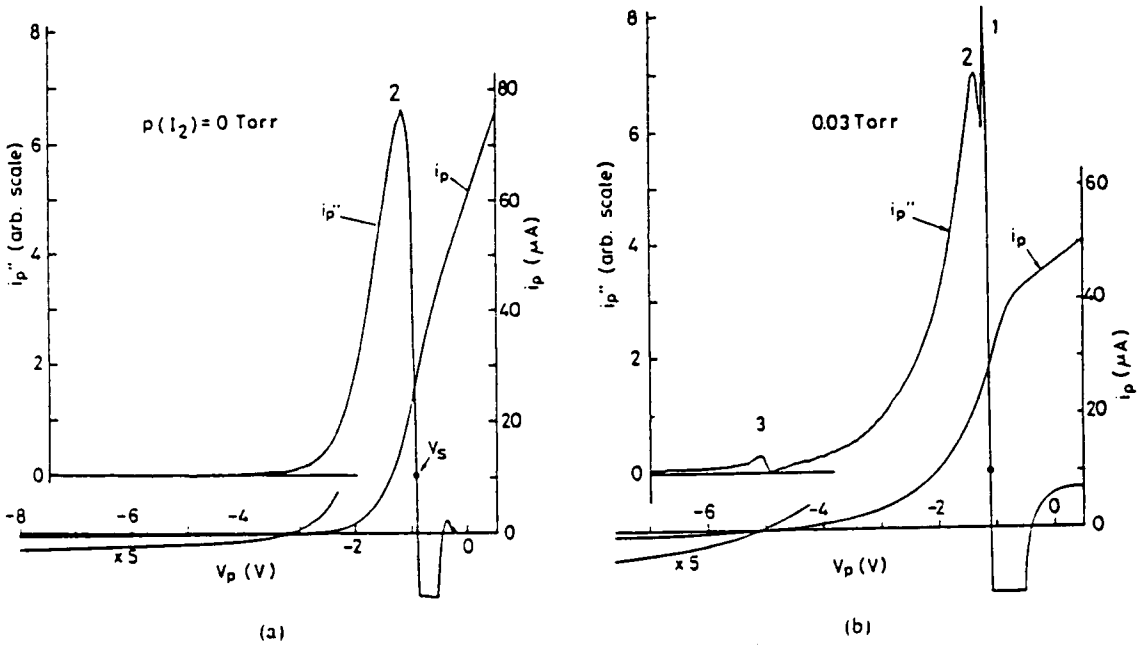


Fig. 20. Negative ion influence on probe characteristic; a) pure argon discharge at p=0.64 Torr, b) the same with 0.03 Torr of iodine (after Amemiya,69).

As one can see, a sharp peak appears near the plasma potential $V_S$ when a small amount of iodine is introduced into the discharge. This peak has been identified as due to negative ions and has been used for calculation in their density $n_-$ and temperature $T_-$.

## 5.7 EEDF measurement in noisy and RF plasmas

Probe measurements and specifically measurements of EEDF in noisy or RF excited plasma run into some serious problems. One of them is evident and refers to the decreasing S/N ratio which finally deteriorates the dynamic range of the measured EEDF or even blocks the measured signal. This kind of problem can be partially overcome by using a filtering and phase detection technique in the ac-differentiating method or the ensemble-averaging technique in the pulse method. Note that in the great majority of plasma experiments, the interfering noise is not random and therefore the use of an averaging technique yields rather limited success in increasing the dynamic range.

The second problem refers to distortions of the probe characteristics and their derivatives caused by non-linear interaction of noise or ac periodical oscillations with the

probe sheath. This kind of distortion cannot be removed by using an S/N improvement technique since the measured signal is already distorted before being processed. Probe characteristic distortions caused by plasma periodic and random oscillations have been studied for some time,73-77. It has been shown that a smoothing of the I/V probe characteristic occurs near the plasma potential if the ac component of the probe voltage is comparable to or larger than the electron temperature (expressed in volts). This effect is similar to distortions which take place at differentiating probe I/V characteristics with large ac voltage.

The influence of the ac probe voltage on EEDF measurement has been studied theoretically and experimentally by Wiesemann,78, Godyak and Oks,79 and Blagoev et al,80. The results of these studies have demonstrated significant second derivative distortions. The main features of these distortions are a widening of the voltage gap between maximum and zero of the second derivative and suppression of its maximum. Sometimes a false maxima can appear on a distorted second derivative. The distortion on the second derivative depends on the kind of undistorted EEDF,79 as well as the shape of the probe interfering voltage,80. Typical distortions in the second derivative measurements caused by an rf voltage artificially introduced into the probe sheath and in the second derivatives obtained in a microwave plasma are shown in Figs. 21 and 22.

To avoid the above mentioned distortion in noisy or rf discharge plasmas, one must eliminate the interfering ac voltage in the probe sheath. This is achieved by various means depending on the frequency spectrum of the interfering probe voltage.

For noisy dc discharges with a noise bandwidth within a hundred KHz, effective noise suppression can be achieved by using an additional tracking probe and associated electronics to pick up the noise signal and introduce it, in the opposite phase, into the probe measurement circuit. This eliminates interfering noise in the probe sheath, providing that the electronics itself does not distort the noise signal. Such an arrangement in EEDF measurement was first implemented by Rayment and Twiddy,24 for compensation of an ac-differentiating voltage drop across the plasma. Later this technique incorporated with an ac- differentiating technique was used for noise suppression by Gulidov et al,82, Kagan et al,83, and Matsumura and Sin-Li Chen,84, see also 85. A block diagram of the experimental setup with a noise suppression circuit and typical results are shown in Fig. 23.

In this arrangement the noise voltage is sensed by the tracking probe 2 and introduced into the measurement circuit by the follower (unity gain amplifier). Thus, the measurement probe 1 is biased by the noise voltage, and the noise voltage

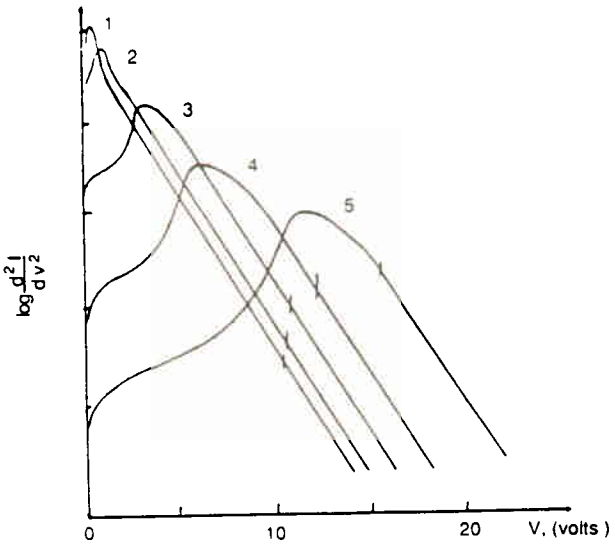


Fig. 21. Second derivatives obtained in dc mercury discharge ($p=1.2.10^{-3}$ Torr) with different amplitude of artificially introduced rf probe voltage V~. Vertical marks show floating potentials. 1)V~=0; 2) 1; 3) 3; 4) 5; 5) 10 volts (after Godyak and Oks,79).

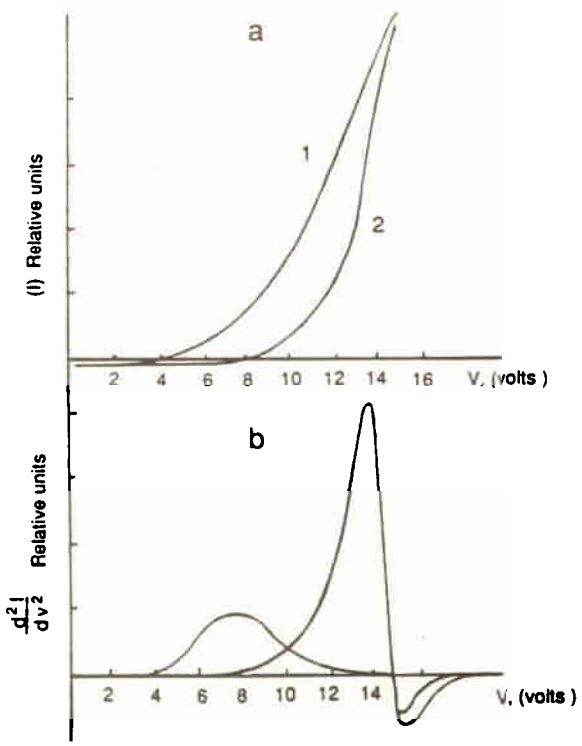


Fig. 22. Probe characteristics and their derivatives obtained in a microwave discharge. 1) distorted and 2) undistorted probe measurements (after Ivanov et al,81).

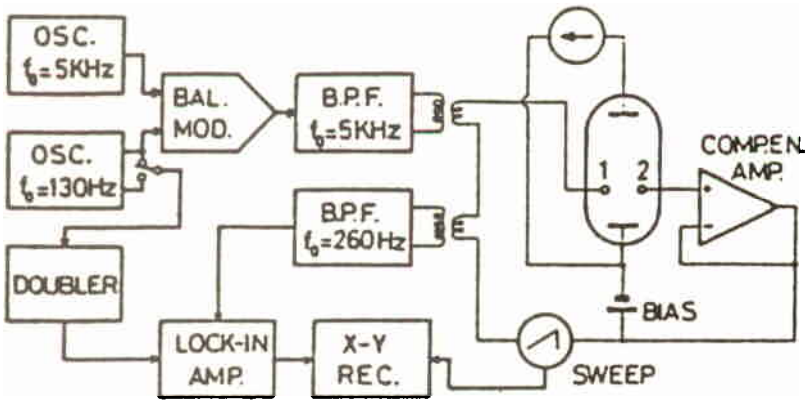


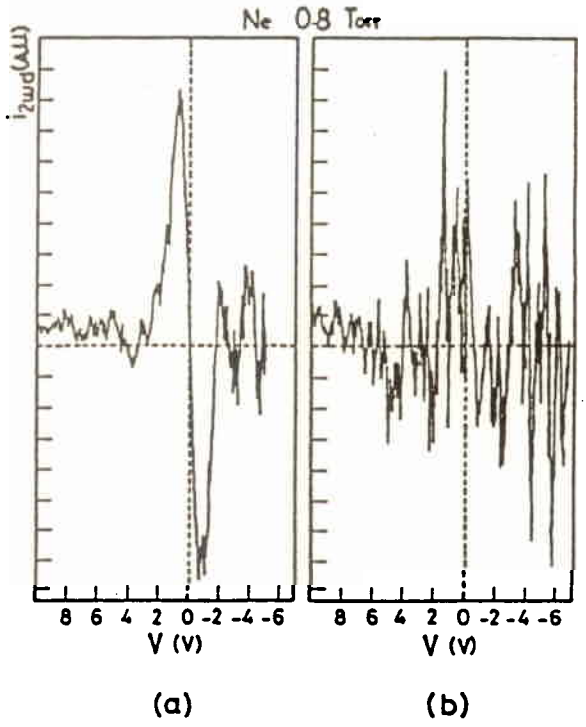


Fig. 23. The block diagram of the experimental setup and the typical results of the second derivative measurement (a) with noise suppression and (b) without noise suppression (after Matsumura and Sin-Li Chen,84).

difference across the measurement probe sheath is compensated. As one can see in Fig. 23, the noise-suppression technique creates an improvement in EEDF measurement, but to achieve the true benefit of noise-cancelling technique, some degree of electronic design expertise is necessary.

The noise suppression technique can cancel not only noise, but also any voltage drop (dc and ac) arising between measurement probe and reference electrode (cathode or anode), providing that the tracking probe is not placed too far from the measurement probe. Since the frequency and phase responses of the described noise suppression circuits are limited, it is impractical to adapt this circuit to probe measurements with rf excited plasmas. Note that to eliminate penetration of rf voltage into the probe sheath from a 13 MHz rf discharge, a large amplitude voltage follower with a time response of 1 ns or less would be required.

To avoid probe measurement distortion in an rf discharge plasma, care should be taken towards proper design of the probe circuit. These have been considered for Langmuir probe applications in rf excited plasmas by Gagne and Cantin,86-87, Godyak and Popov,88, Mosburg et al,89 and Braithwait et al,90.

Two approaches are known to eliminate rf voltage within the probe sheath. The first is to use rf filters to allow the probe to track the rf plasma potential,86,88, and the second is to drive the probe with an auxiliary rf voltage whose amplitude and phase are adjusted to be equal to the rf plasma potential,90.

In application to the EEDF measurement, a filtering technique has been used by Ivanov et al,81 Godyak and Oks,91, and Vagner and Ignat'ev,92. Probe measurement circuits have been connected with probes via resonant filters tuned to the fundamental and second harmonic of the driving frequency. Note that a considerable second harmonic component exists in the plasma potential of the rf discharge,86. It is also very important for successful use of this technique that the filter impedance be much larger than the probe sheath impedance,76.

An RF driven probe technique to eliminate rf distortion in EEDF measurement has been used by Cox et al,93. No attempt was made in their experiment to compensate the second harmonic of the plasma potential. This probably was the reason for some of the exotic shapes for the EEDF's obtained in their experiment.

It seems that proper design of the probe circuit remains the most complicated, but solvable, problem in EEDF measurements of rf plasmas.

The problems considered above which one may encounter in performing an EEDF measurement can be overcome with available technology. A high quality EEDF measurement with reasonable energy resolution and large dynamic range: (up to 60-80 db)

can be achieved using a digital scope or a waveform analyzer with ensemble-averaging option, together with relatively simple analog electronics. An example of such a measurement is shown in Fig. 24.

Here, the second derivative is obtained with a setup developed at the Sylvania Lighting Center. The arrangement is based on a combination of a fast pulse-differentiating technique with ensemble averaging, a noise suppression feedback circuit, and an automated cleaning of the probe during the measurement. This system has been briefly reported in 94 and will be described in detail elsewhere.

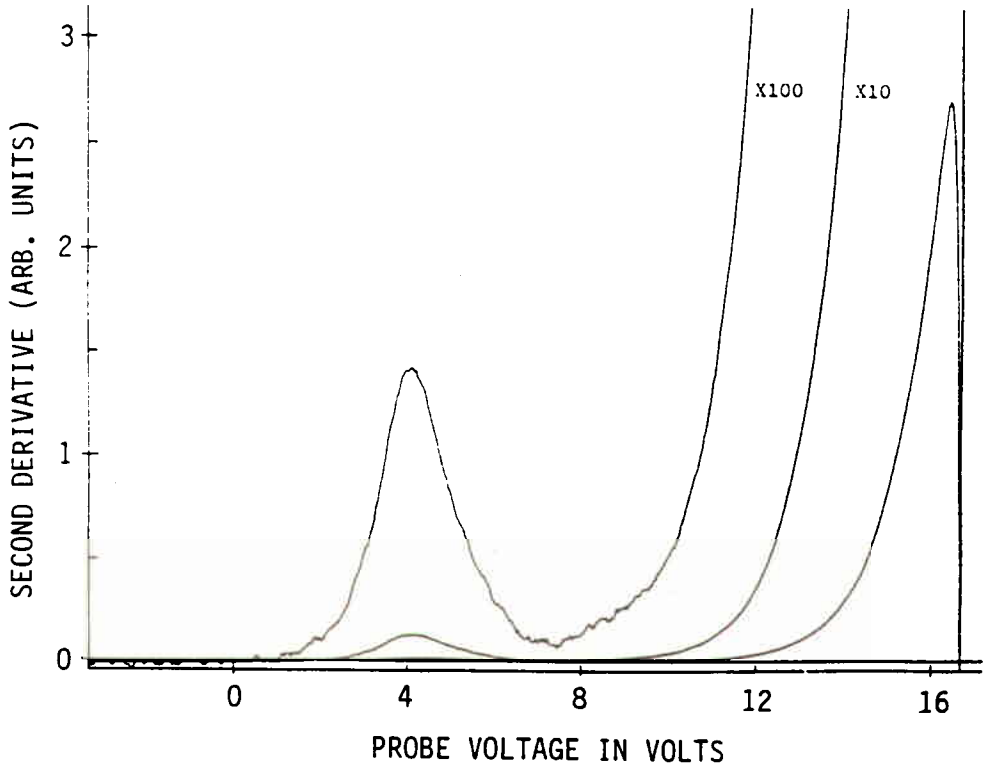


Fig. 24. Second derivative obtained in the cathode glow of the neon-mercury arc discharge at the distance of 6mm from a thermionic cathode (author's measurement).

REFERENCES


1. I. Langmuir, "Collected Works of Irving Langmuir", ed. G. Suits, Vol. 4, New York 1961. Gen. Elec. Rev., 27, 449, 1924; Phys. Rev. 28, 727, 1926.
2. Yu M. Kagan and V. I. Perel, Soviet Phys. Usp., 6, 763 1964.
3. F. Chen, "Plasma Diagnostic Technique", R. H. Huddlstone and S. L. Leonard, ed., Academic Press, New York, 1965.
4. L. Schott, "Plasma Diagnostics", W. Lochte-Holtgreven, ed., North Holland Publishing Co., Amsterdam, 1968.
5. O. V. Kozlov, "The Electric Probe in Plasma", (in Russian), Atomizdat, Moscow, 1969.
6. Y. D. Swift and M. J. R. Schwar, "Electrical Probes for Plasma Diagnostics", American Elsevier, New York, 1969.
7. J. F. Waymouth, "Electric Discharge Lamps", MIT Press, Cambridge, MA 1971.
8. P. M. Chang, L. Talbot, K. J. Touryan "Electric Probes in Stationary and Flowing Plasmas", Springer-Verlag, Berlin, Heidelberg, N.Y. 1975
9. B. E. Cherrington, "Plasma Chemistry and Plasma Processing", 2, 113, 1982.
10. M. J. Druyvesteyn, "Der Niedervoltbogan", Z. Phys, 64, 781, 1930.
11. V. M. Milenin and N. A. Timofeev, "Spectroscopiya Gazorazriydnoi Plazmy" (in Russian), ed. Leningrad University, Leningrad, 1980.
12. R. Sloan and McGregor, Phill. Mag. 18, 193, 1934.
13. L. A. Gavalass, Yu. M. Kagan, G. M. Malyshev and V. L. Fedorov, DAN SSSR, 79, N2, 1951.
14. G. M. Malyshev and V.L. Fedorov, DAN SSSR 93, N2 1953
15. P.L.V. Boyd and N. D. Twiddy, Proc. Roy. Soc., 250, 260, 1959.
16. G. A. Branner, E. M. Friar, and G. Medicus, Rev. Sci. Instr., 34, 231, 1963.
17. K. F. Schoenberg, Rev. Sci. Instr. 51, 1159, 1980.
18. E. Alexeff and D. F. Howell, J. Appl. Phys, 40, 4877, 1969.
19. K. Wiesemann, Proc. IX Int'l. Conf. Phenom. Ionized Gases, 615, Bucharest, 1969.
20. K. F. Schoenberg, Rev. Sci. Instr., 49, 1377, 1978.
21. D. R. Nordlund and O. P. Breaux, Rev. Sci. Instr., 42, 248, 1972; Technial Reort AFAL-TR-71-294 Air Force Avionics Laboratory, AFSC, Wright-Patterson AFB, Ohio 1971.
22. M. B. Hopkins and W. G. Graham, Rev. Sci. Instr., 57, 2210, 1986.
23. M. B. Hopkins and W. G. Graham, J. Phys. D:Appl. Phys, 20, 838, 1987.
24. S. W. Rayment and N. D. Twiddy, Brit. J. Appl. Phys. (J. Phys. D) 2, 1747, 1969.
25. O. N. Oreshak, A. F. Stepanov and V. A. Stepanov, Sov. Phys.-Tech. Phys., 16, 93, 1971.
26. S. W. Rayment and N. D. Twiddy, J. Phys D:Appl. Phys, 6, 2242, 1973.
27. M. Adriaansz, J. Phys E:Instr., 6, 743, 1973.

28. K. Shimizu and H. Amemiya, J. Phys. E:Sci. Instr., 10, 389, 1977.
29. Yu. M. Kagan and V. I. Perel, Sov. Phys.-Tech. Phys. 13, 141, 1968.
30. N. A. Vorobjeva, V. M. Zaharova and Yu. M. Kagan, IX Int'l. Conf. Phenom. Ionized Gases, 620, Bucharest, 1969.
31. K. Wiesemann, Ann. Phys. (Leipzig) 23, 275, 1969.
32. D. Andersson, J. Phys. D:Appl. Phys. 10, 1549, 1977.
32. J. E. Allen, J. Phys. D:Appl. Phys. 11, 135, 1978.
34. A. I. Lukovnikov, Sov. Phys.-Tech. Phys. 18, 936, 1974.
35. V. L. Fedorov, Sov. Phys.-Tech. Phys. 30, 584, 1985.
36. A. P. Mezentsev, A. S. Mustafaev and V. L. Fedorov, Sov. Phys.-Tech Phys. 30, 322, 1985.
37. V. L. Fedorov and A. P. Mezentsev, Sov. Phys.-Tech. Phys. 32, 363, 1987.
38. A. . Mezentsev and A. S. Mustafaev, Sov. Phys.-Tech. Phys. 30, 1319, 1985.
39. J. F. Waymouth, Phys. Fluids, 7, 1893, 1964; Phys. Fluids, 9, 801, 1966.
40. H. J. Cornelissen, and H.J.H. Merks-Eppingbroek, J. Appl. Phys. 59, 2324, 1986.
41. J. F. Waymouth, J. Appl. Phys. 37, 4493, 1966.
42. A. I. Lukovnikov and M. Z. Novgorodov, Sov. Phys.-Tech. Phys. 16, 1931, 1972.
43. L. M. Volkova, A. M. Devyatov and M. A. Sherif, Sov. Phys.-Plasma Phys. 3, 1156, 1977.
44. E. Berger and A. Heisen, J. Phys. D: 8, 629, 1975.
45. H. Amemiya and K. Shimizu, J. Phys. E:Sci. Instr., 12, 581, 1979.
46. R. M. Howe, J. Appl. Phys., 24, 881, 1953.
47. G. Wehner and Medicus, J. Appl. Phys., 23, 1035, 952.
48. M. A. Easley, J. Appl. Phys., 22, 590, 1951,
49. R. J. D'Arcy, J. Phys. D:Appl. Phys., 7, 1391, 1974.
50. W. Verweij, Philips Res. Rep., 2, 1961.
51. H. Amemiya and K. Wiesemann, J. Phys. D:Appl. Phys., 5, 1829, 1972.
52. M. Venugopalan, Plasma Chemistry and Plasma Proc., 3, 275, 1983.
53. R. Y. D'Arcy, J. Phys. D:App. Phys., 7, 1974.
54. J. F. Waymouth, J. Appl. Phys., 30, 1404, 1959.
55. K. Wiesemann, Ann. Phys. (Leipzig) 27, 303, 1971.
56. H. B. Blagoev, Yu. M. Kagan, N. B. Kolokolov and R. I. Lyagushchenko, Sov. Phys.-Tech. Phys., 20, 360, 1975.
57. Yu. M. Kagan, N. B. Kolokolov, P. M. Pramatorov and M. A. Petrun'kin, Sov. Phys.-Tech. Phys., 22, 687, 1977.
58. V. I. Demidov and N. B. Kolokolov, Sov. Phys.-Tech. Phys., 28, 533, 1981.
59. L. M. Volkova, V.I. Demidov, N. B. Kolokolov and E. A. Kral'kina, Sov. Phys.-Tech. Phys., 28, 583, 1983.
60. K. Wiesemann, Z. Physik, 219, 462, 1969.
61. V. I. Demidov, N. B. Kolokolov and O. G. Toronov, Sov. Phys.-Tech. Phys., 29, 230, 1984.
62. A. N. Lukovnikov and M. Z. Novgorodov, Short Reports on Physics, FIAN, 1, 27, 1971 (in Russian).
63. S. D. Vagner and B. K. Ignat'ev, Sov. Phys.-Tech. Phys., 25, 558, 1977.

64. V. A. Dovzhenko, A. P. Ershov and G. S. Solntsev, Sov. Phys.-Tech. Phys., 19, 851, 1974.
65. E. R. Mosburg, Rev. Sci. Instr., 52, 1182, 1981.
66. J. G. Laframboise, "Rarefied Gas Dynamics", Vol. 11, ed. J. H. de Leeuw, Academic Press, New York, 1965, Univesity of Toronto, Institute for Aerospace Study, Report No. 100, 1966.
67. K. D. Asvadurov and I. A. Vasil'eva, Sov. Phys.-Tech. Phys., 20, 996, 1975.
68. J. B. Thompson, Proc. Phys. Soc., 73, 818, 1959.
69. H. Amemiya, J. Phys. Soc. Japan, 57, 887, 1988.
70. H. Amemiya, J. Phys. Soc. Japan, 55, 169, 1985.
71. H. Amemiya and Y. Sakamoto, Japan J. Appl. Phys., 26, 1170, 1987.
72. M. Amemiya, Japan J. Appl. Phys., 25, 595, 1986.
73. A. Garscadden and K. G. Emeleus, Proc. Phys. Soc., 79, 535, 1962.
74. F. W. Crawford, J. Appl. Phys., 34, 1963.
75. A. Boschi and F. Magistrelli, Nuovo Cimento, 29, 487, 1963.
76. V. A. Godyak, "Soviet Radio Frequency Discharge Research," ed. Delphic Ass., Falls Church, VA, 1986.
77. K. Matsumoto and M. Sato, J. Appl. Phys., 54, 1781, 1983.
78. K. Wiesemann, Phys. Letters, 25A, 701, 1967.
79. V. A. Godyak and S. N. Oks, Sov. Phys.-Tech. Phys., 24, 784, 1980.
80. A. B. Blagoev, V.I. Demidov, N. V. Kolokolov and O. G. Toronov, Sov. Phys.-Tech. Phys., 26, 1179, 1981.
81. Yu. A. Ivanov, Yu. A. Lebedev and L. S. Polak, Sov. Phys.-Tech. Phys., 21, 830, 1976.
82. S. S. Gulidov, Yu. M. Kagan, N. B. Kolokolov and V. M. Milenin, Sov. Phys.-Tech. Phys. 14, 993 1970.
83. Yu. M. Kagan, N. B. Kolokolov, R. I. Lyagushchenko, V. M. Milenin and A. M. Mirzabekov, Sov. Phys. - Tech. Phys 16, 561, 1971.
84. S. Matsumura and Sin-Li Chen, Rev. Sci. Instr., 50, 1425, 1979.
85. H. M. Musal, J. Appl. Phys. 41, 2605, 1970.
86. R.R.J. Gagne and A. Cantin, J. Appl. Phys. 43, 2639, 1972.
87. A. Cantin and R.R.J. Gagne, Third Intern. Conf. on Gas Disch., 625, Longdon, 1974.
88. V. A. Godyak and O. A. Popov, Sov. Phys.-Tech. Phys., 22, 461, 1977.
89. E. R. Mosburg, R. C. Kerns and J. R. Abelson, J. Appl. Phys., 54, 4916, 1983.
90. N. St. J. Braithwait, N.M.P. Benjamin and J. E. Allen, J. Phys. E: Instrum 20, 1046, 1987.
91. V. A. Godyak and S. N. Oks, Sov. Phys.-Tech. Phys. 24, 1255, 1979.
92. S. D. Vagner and B. K. Ignat'ev, Sov. Phys.-Tech. Phys., 28, 398, 1983.
93. T. I. Cox, V.G.I. Deschmukh, D. A. Hope, A. J. Hydes, N. St. J. Braithwait and N.M.P. Benjamin, J. Phys. D: Appl. Phys. 20, 820, 1987.
94. V. Godyak, R. Lagushenko and J. Maya, Phys-Rev.A, 38, 2044, 1988.